JOURNAL OF GEOPHYSICAL RESEARCH, VOL. 104, NO. D24, PAGES 31,127–31,143, DECEMBER 27, 1999

Model-based estimation of the global carbon budget and its uncertainty from carbon dioxide and carbon isotope records

Haroon S. Kheshgi

Corporate Research Laboratories, Exxon Research and Engineering Company, Annandale, New Jersey

Atul K. Jain and Donald J. Wuebbles

Department of Atmospheric Sciences, University of Illinois, Urbana

Abstract. A global carbon cycle model is used to reconstruct the carbon budget, balancing emissions from fossil fuel and land use with carbon uptake by the oceans, and the terrestrial biosphere. We apply Bayesian statistics to estimate uncertainty of carbon uptake by the oceans and the terrestrial biosphere based on carbon dioxide and carbon isotope records, and prior information on model parameter probability distributions. This results in a quantitative reconstruction of past carbon budget and its uncertainty derived from an explicit choice of model, data-based constraints, and prior distribution of parameters. Our estimated ocean sink for the 1980s is 17 $\pm$ 7 Gt C (90% confidence interval) and is comparable to the estimate of 20 $\pm$ 8 Gt C given in the recent Intergovernmental Panel on Climate Change assessment [*Schimel et al*., 1996]. Constraint choice is tested to determine which records have the most influence over estimates of the past carbon budget; records individually (e.g., bomb-radiocarbon inventory) have little effect since there are other records which form similar constraints.

1. Introduction

Projections of future global climate change have led to the consideration of actions intended to limit the buildup of greenhouse gases in the atmosphere [*United Nations* (UN), 1992]. Uncertainty in projections of the climate response to future emissions of greenhouse gases remains a critical factor in determining when and what actions are taken. One contributor in the overall uncertainty is the relation between emissions of carbon dioxide and the resulting atmospheric concentration of carbon dioxide determined from the behavior of the carbon cycle within the ocean-biosphere-atmosphere system. Emitted carbon dioxide increases the atmospheric concentration, which is then thought to increase the rate at which carbon is taken up, for example, by dissolution in the oceans and by enhanced growth of the terrestrial biosphere. Models used to project future concentrations of atmospheric carbon dioxide can approximate the behavior of the Earth's past carbon cycle, at least to the extent we have observations and measurements that constrain its possible past behavior. Global carbon cycle exhibits exchanges of carbon between the biosphere and atmosphere and the oceans and atmosphere at annual rates ($\sim$100 billion tons of carbon per year each) that far exceed the annual emissions of carbon dioxide by the burning of fossil fuels ($\sim$6 billion tons of carbon per year). Possible shifts in the exchanges of carbon between the Earth's reservoirs in unexpected ways remain a source of uncertainty in projections of the behavior of future carbon cycle that is difficult to assess. Nevertheless, the accuracy with which we can reconstruct the workings of the past carbon cycle forms an important factor leading into an assessment of the uncertainty of projections of future atmospheric response.

Paper number 1999JD900992.
0148-0227/99/1999JD900992$09.00

Many estimates of the past global carbon budget have been made, as reviewed by *Siegenthaler and Sarmiento* [1993] and *Schimel et al*. [1995]. The sink of carbon dioxide into the oceans has been estimated by models that attempt to reproduce ocean circulation and transport [*Maier-Reimer*, 1993; *Maier-Reimer and Hasselmann*, 1987; *Sarmiento et al*., 1992] and by parametric models that use ocean concentrations of radiocarbon for model calibration or validation [*Broecker and Peng*, 1994; *Jain et al*., 1995; *Oeschger et al*., 1975; *Siegenthaler and Joos*, 1992]. The uncertainty of the ocean sink contribution to the global carbon budget has been estimated using ocean carbon cycle models [*Schimel et al*., 1995; *Siegenthaler and Sarmiento*, 1993] for which the ocean inventory of bomb radiocarbon [*Broecker et al*., 1980, 1995] has been used for model validation. *Heimann and Maier-Reimer* [1996], *Quay et al*. [1992], and *Tans et al*. [1993] have considered the effect of carbon 13 constraints on the global-average ocean sink of carbon as an alternative to radiocarbon constraints. The anthropogenic signal in the ocean has also been estimated from the observations from changes in preformed carbon using techniques originally proposed by *Brewer* [1978] and *Chen and Millero* [1979] and recently refined by *Gruber et al*. [1996]. In addition, tritium and CFCs have been used to calibrate or validate various regions of ocean models [*Bullister*, 1989; *Doney et al*., 1993]; for example, *Mensh et al*. [1998] used CFCs to calibrate the high latitudinal deep ocean component of their carbon cycle model. *Keeling et al*. [1996] have considered trends in atmospheric oxygen concentration as a constraint on the recent carbon budget.

The range of results of different models was considered as one measure of model uncertainty [*Bruno and Joos*, 1997; *Enting et al*., 1994; *Schimel et al*., 1996], even though the results of these models are not all consistent with isotopic records as shown by *Jain et al*. [1995]. Furthermore, a generic weakness of using model intercomparisons to estimate uncertainty is that the model results that are intercompared are usually the "best

guess" results of each model, and the relation between best guess results and the uncertainty of the mean estimate is unclear. However, model intercomparisons can give indications of differences in model results which cannot be simulated by variation of existing model parameters due to differences in model structure (e.g., resolution, mechanisms, and formulation); model structure uncertainty is an important consideration in model-based estimation of uncertainty.

In this study we consider the extent to which measured concentrations of carbon dioxide and carbon isotopes and estimates of emissions determine the past carbon budget. We do this by applying Bayesian estimation of the parameters of a global carbon cycle model using data-based records as constraints. In this study we consider only aggregated records of carbon dioxide and carbon isotopes for the global atmosphere, oceans, and ocean mixed layer. Spatially resolved data do, however, provide additional information that could be used in comparisons to spatially resolved models to further our quantitative understanding of carbon cycle. Including records of, for example, oxygen, tritium, and CFCs as well as considering other model structures would also add more information and thus lead to better estimates and is recommended for future studies. In section 2 we describe the method of Bayesian parameter estimation as applied to this problem. In this application of Bayesian parameter estimation a carbon cycle model and a prior probability distribution of model parameter values are specified. The carbon cycle model is designed to have sufficient degrees of freedom to well represent the past carbon budget. These degrees of freedom are characterized by a set of parameters or model inputs. The globally aggregated model for carbon cycle used in this analysis is described in section 3 and is the same model that has been used both to reconstruct past records [*Jain et al*., 1995, 1996, 1997] and to make future projections of the atmospheric response to emissions [*Jain et al*., 1994; *Kheshgi et al*., 1996, 1997. The prior estimate of model parameters is based on information about the parameters prior to application of constraints. Model parameters include model inputs which are well known, for example, CO_2 emission rates from the burning of fossil fuels, for which we specify a narrow prior probability distribution, as well as parameters that are not well known, e.g., the effective vertical diffusivity of the oceans, for which we specify a wide prior probability distribution. In section 4, model inputs and parameters are discussed, and a base-case set of prior estimates is defined. Data-based constraints on model outputs are used in addition to prior parameter estimates in Bayesian parameter estimation in order to calculate a posterior (i.e., after imposition of the constraints) estimate of the model parameters which will have a narrower probability distribution than the prior estimate. In section 5 we describe a base-case set of observation-based measures of the distribution of carbon dioxide and carbon isotopes which are used as constraints on the model output. Constraints based on data analyses exhibit varying degrees of accuracy which we represent by a specified probability distribution. Posterior estimates are calculated, and results are reported in section 6.

Effects of the choice of constraints and prior parameter estimates are tested to determine which records have the most influence over estimates of the past carbon budget. The sensitivity of posterior estimates and the reconstructed carbon budget to prior parameter estimates and constraints is examined by applying alternative sets (other than the base-case sets) of priors and constraints. We make comparisons between our approach and previous analyses of the uncertainty in the reconstruction of the past carbon budget by examining the effect of subsets of constraints on posterior estimates of model outputs and parameters. We discuss, in the final section, conclusions that can be drawn from this study and implications for the determination of the uncertainty of future projections of the atmospheric response to emission.

2. Bayesian Framework for Estimation of Uncertainty

The method by which we apply the data constraints is Bayesian parameter estimation [*Press*, 1989], which we describe in this section. Let α be an m-dimensional vector of the true model parameters which we will try to estimate, and let $M(\alpha)$ be a d-dimensional vector of model predictions, which obviously depends on α. Let D be a d-dimensional vector of data, differing from M by error $\gamma(\alpha)$ which is, in general, an α-dependent random d-vector. Then, the following error model applies:

$$D = M(\alpha) + \gamma(\alpha). \tag{1}$$

We assume that the errors are modeled statistically; that is, the conditional probability density of γ for known α, $P_\gamma(\gamma|\alpha)$, has been determined. Then if α is known, we have the conditional probability density of D given by

$$P_D(D|\alpha) = P_\gamma(D - M(\alpha)|\alpha) \equiv P_\gamma(\gamma|\alpha). \tag{2}$$

In the Bayesian framework, α is considered a random vector and this device allows incorporation of prior knowledge of the likely behavior of parameters through a prior probability density $\bar{P}_\alpha(\alpha)$. This distribution expresses our state of knowledge of the values of the model parameters before the data constraints are applied.

From the law of total probability the unconditional probability density of the data is

$$\bar{P}_D(D) = \int_{\Omega_\alpha} P_D(D|\alpha)\bar{P}_\alpha(\alpha)\, d\alpha. \tag{3}$$

From Bayes' rule, the probability density of the unknown vector of parameters α, after the data have been obtained, is

$$P_\alpha(\alpha|D) = \frac{P_D(D|\alpha)\bar{P}_\alpha(\alpha)}{\bar{P}_D(D)}, \tag{4}$$

where $P_\alpha(\alpha|D)$ is the posterior probability density of α and contains all known information about the parameters after the data constraints have been incorporated with the prior information.

In this study we apply some simplifying assumptions to the analysis. First, we assume that the probability distribution of both the data and the prior estimates of the model parameters are Gaussian. This allows us to characterize uncertainty by a covariance matrix. While the actual probability distribution might not actually be Gaussian, the probability distribution of the data and the prior parameter estimates are not well known, making the specification of a detailed probability distribution quite subjective. Second, we assume that the model response is linearly dependent on model parameters in the neighborhood of the prior estimate of the parameters. While the model response, in general, is not linear, this simplifies the analysis and interpretation of results. This approach can, nonetheless,

be extended to consider a nonlinear model response using Monte Carlo methods; however, estimation of the posterior probability distribution using such methods [*Duran and White*, 1995] with the number of parameters considered here would be extremely computationally intensive. To examine the effects of nonlinearity, the estimation problem could potentially be simplified (reducing the number of parameters and constraints by, for example, principal component analysis) based on the linear analysis reported here; nonlinear effects will likely be critical if parameter estimates were used to examine the uncertainty of projections of the future atmospheric response to emissions. If the model response is linear, and the probability distribution of both the data and the prior estimates of the model parameters is Gaussian (assumed), then the posterior probability distribution of the model parameters will also be Gaussian.

The prior probability density of parameters is specified to be the Gaussian distribution

$$\bar{P}_{\alpha}(\alpha) = \frac{\exp\left[-1/2(\alpha - \alpha_{\text{prior}})^T C_{\text{prior}}^{-1}(\alpha - \alpha_{\text{prior}})\right]}{\sqrt{\det\,(2\pi C_{\text{prior}})}}, \quad (5)$$

where C_{prior} is the covariance matrix of the prior parameter estimate, and α_{prior} is the mean. We assume that the errors in the prior estimate of the parameters are not correlated with each other, making C_{prior} a diagonal matrix with the diagonal entries σ^2_{prior} where σ_{prior} is the standard error.

The probability density of the error is, likewise, specified to be the Gaussian distribution

$$P_D(D|\alpha) = \frac{\exp[-1/2(D - M(\alpha))^T C_{\text{error}}^{-1}((D - M(\alpha)))]}{\sqrt{\det(2\pi C_{\text{error}})}} \quad (6)$$

where C_{error} is the covariance matrix of the error between the model result and the data, and the mean of the error is assumed to be zero. We first assume that the error is predominantly due to (measurement) error in the data. This is an important assumption in this study. A deficient model formulation should be expected to not be able to represent the true (yet unknown) values of the constraints. Alternative models could be used to test for sensitivity to this assumption. We then assume that the covariance matrix C_{error} is independent of α. We assume that data errors are not correlated to each other, making C_{error} a diagonal matrix with the diagonal entries equal to σ^2_{data}, the square of the standard error σ_{data}.

Next, we approximate the model as its linearization about the mean value of the prior estimate α_{prior} to give

$$\mathbf{M} \cdot (\alpha - \alpha_{\text{prior}}) + M(\alpha_{\text{prior}}) \approx M(\alpha) \quad (7)$$

where $\mathbf{M}$ is the model sensitivity matrix to parameters α about the mean value of the prior estimate

$$\mathbf{M} \equiv \left.\frac{\partial M(\alpha)}{\partial \alpha}\right|_{\alpha_{\text{prior}}}, \quad (8)$$

which is generated by finite differences of model results.

Finally, (1)–(8) are combined to give the posterior estimate which also has a Gaussian distribution. The mean value of the posterior estimate is given by

$$\alpha_{\text{posterior}} = \alpha_{\text{prior}} + C_{\text{posterior}}[\mathbf{M}^T C_{\text{error}}^{-1}(D - M(\alpha_{\text{prior}}))], \quad (9)$$

where the posterior covariance is

$$C_{\text{posterior}} = [\mathbf{M}^T C_{\text{error}}^{-1}\mathbf{M} + C_{\text{prior}}^{-1}]^{-1}. \quad (10)$$

The posterior covariance matrix gives the posterior estimate of the uncertainty of model parameters. Note that the second term in (9) is associated with the data constraints, while the first term incorporates only prior information on parameter values. The sum gives the proper weighting according to our knowledge of statistical error. Thus parameters well identified by data constraints will be insensitive to the prior distribution. However, parameters not well determined by the data will not wander during estimation, since they are constrained by the prior density.

The improved estimate of model outputs is found by evaluating the model with the mean value of the posterior estimates of model parameters, $M(\alpha_{\text{posterior}})$ or, alternatively, approximating the model as being linearly dependent on the model parameters about the mean prior estimate of parameters, as was done in (7):

$$M(\alpha_{\text{posterior}}) \approx \mathbf{M} \cdot (\alpha_{\text{posterior}} - \alpha_{\text{prior}}) + M(\alpha_{\text{prior}}). \quad (11)$$

To find the posterior estimate of the uncertainty in model outputs, the covariance matrix for the model outputs is calculated from

$$C_{\text{output}} = \mathbf{M} C_{\text{posterior}} \mathbf{M}^T. \quad (12)$$

Model outputs include model predictions of data, as given by (1), and can also be extended to include quantities desired as outputs (augmenting D to contain desired quantities) for which there is no data-based estimate; the uncertainty of these quantities with which D has been augmented is infinitely large, which is approximated in computations by specifying a large number for the corresponding diagonal terms in C_{error}. The associated diagonal terms of the posterior covariance for the outputs C_{output} calculated using (12) are, nevertheless, finite.

3. Parametric Model for Global Carbon Cycle

Bayesian parameter estimation is applied to the linearized form (equations (7)–(9)) of the parameterized model for a globally aggregated carbon cycle which was used by *Jain et al.* [1996] to reconstruct the past carbon cycle and isotopic variations in the atmosphere and oceans, which is described in section 3.1. These reconstructions of carbon budget depend on a set of model parameters and model inputs which are not necessarily known with precision. To make these reconstructions, model parameters were calibrated [*Jain et al.*, 1996] to match a subset of the observation-based constraints considered in this study; and these parameter values are used as the mean prior estimate of model parameters in this study (see Table 1) which also serves as the point in parameter space about which the model is linearized; see (7) and (8) as described in section 3.2. Note that this model reconstruction will differ from the budget based on the posterior estimate of model parameters given in section 6. Finally, in section 3.3 we discuss degrees of freedom designed into the model, which will be important for interpreting results.

3.1. Model Description

The model of the global carbon cycle depicted in Figure 1 is used to simulate the exchange of carbon dioxide, ^{13}C and ^{14}C between the atmosphere, reservoirs of carbon in the terrestrial biosphere, and the ocean column and mixed layer [*Jain et al.*, 1995, 1994, 1996; *Kheshgi et al.*, 1996]. The model consists of a homogeneous atmosphere, an ocean mixed layer and land-

Table 1. Prior and Posterior Estimates of Model Parameters

Description of Model Parameters	Prior Estimates of Model Parameters Mean Value ± 90% Confidence Interval	Posterior Estimates of Model Parameters Mean Value ± 90% Confidence Interval
1. Fossil emission (1765–1980)	158 ± 20 Gt C	158.54 ± 18.40 Gt C
2. Fossil emission (1980–1990)	55 ± 5 Gt C	55.17 ± 4.72 Gt C
3. Land use emission (1765–1980)	133 ± 100 Gt C	110.48 ± 70.13 Gt C
4. Land use emission (1980–1990)	11 ± 11 Gt C	9.31 ± 8.55 Gt C
5. Average annual fossil fuel ^{13}C content (1765–1990)	−24.7 ± 2.2‰	−24.9 ± 2.1‰
6. ^{14}C atmospheric inventory (1950–1965)	2.54 ± 0.25 × 10^{28} atoms	2.58 ± 0.10 × 10^{28} atoms
7. ^{14}C atmospheric inventory (1965–1990)	−1.54 ± 0.15 × 10^{28} atoms	−1.52 ± 0.06 × 10^{28} atoms
8. Translocation Q_{10}	2. ± 4°C	2.06 ± 3.83°C
9. Respiration Q_{10}	2. ± 4°C	1.63 ± 3.60°C
10. NPP Q_{10}	1.4 ± 3°C	1.48 ± 2.98°C
11. NP Q_{10}	1.53 ± 3°C	1.47 ± 3.00°C
12. Fractionation factor (atmosphere to biosphere)	0.9821 ± 0.005	0.9833 ± 0.0049
13. Fractionation factor (atmosphere to ocean)	0.9982 ± 0.0003	0.9982 ± 0.0003
14. Fractionation factor (ocean to atmosphere)	0.9895 ± 0.0003	0.9895 ± 0.0003
15. Fractionation factor (ocean to marine biosphere)	0.9770 ± 0.005	0.9770 ± 0.0050
16. Fertilization factor, β	0.39 ± 0.8	0.37 ± 0.52
17. Upwelling velocity	3.5 ± 20 m/yr	0.25 ± 7.55 m/yr
18. Vertical diffusivity	4.7 ± 20 × 10^3 m^2/yr	4.90 ± 1.25 × 10^3 m^2/yr
19. Ocean NPP	8.5 ± Gt C/yr	7.48 ± 6.18 Gt C/yr
20. Mixed layer depth	75 ± 45 m	72.97 ± 44.16 m
21. Atmospheric rate of exchange, k_a	0.109 ± 0.3 yr^{-1}	0.11 ± 0.02 yr^{-1}
22. Ocean parameter π_c	0.5 ± 2.	0.07 ± 1.36
23. Apparent climate sensitivity	2.5 ± 5°C	1.91 ± 1.12°C
24. Cosmogenic generation of ^{14}C	2. ± 0.5 atom/cm^2/s	2.01 ± 0.03 atom/cm^2/s
25. Terrestrial NPP (1765)	62 ± 30 Gt C/yr	57.79 ± 28.97 Gt C/yr
26. Preindustrial CO_2 concentration (1765)	278 ± 10 ppm	278.05 ± 4.95 ppm

Mean values and 90% confidence intervals of Gaussian distributions are shown. Posterior estimates of model parameters after application of the full set of constraints are listed in Table 2.

biosphere boxes, and a vertically resolved upwelling-diffusion deep ocean. The detailed description of the ocean and land-biosphere components of this model are given by *Jain et al*. [1995] and *Kheshgi et al*. [1996], respectively. In our model the thermohaline circulation is schematically represented by polar bottom-water formation, with the return flow upwelling through the one-dimensional (1-D) water column to the surface ocean from where it is returned, through the polar sea, as bottom water to the bottom of the ocean column, thereby completing the thermohaline circulation. The response of bottom-water carbon concentration to changes in the mixed layer concentration is modeled parametrically by the parameter π_c as described in detail by *Jain et al*. [1995]. A marine biosphere source term is included in the deep sea associated with the oxidation of the organic debris exported from the mixed layer where it is produced by photosynthesis [*Jain et al*., 1995; *Volk and Hoffert*, 1985].

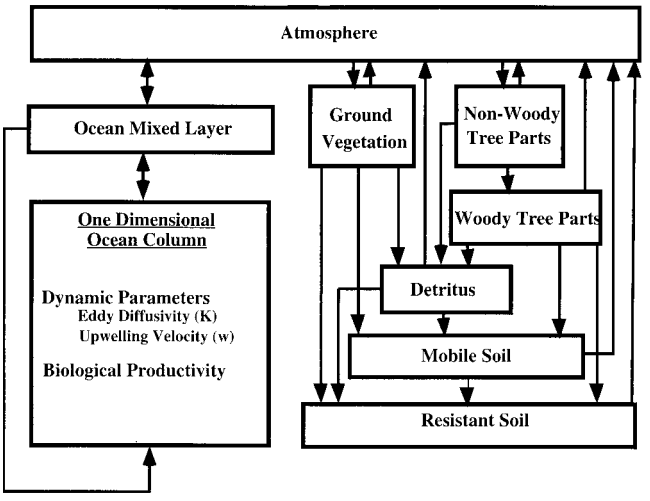

Figure 1. Schematic diagram of the coupled atmosphere-ocean-biosphere model for the global carbon cycle.

To estimate terrestrial biospheric fluxes, a six-box globally aggregated terrestrial biosphere submodel is coupled to the atmosphere box (Figure 1). The terrestrial biosphere model is made up of six boxes that represent ground vegetation, non-woody tree parts, woody tree parts, detritus, mobile soil with a turnover time 70 years, and resistant soil with a turnover time 500 years. The mass of carbon contained in the different reservoirs and their turnover times as well as the rates of exchange between them have been based on the analysis by *Harvey* [1989a] and *Kheshgi et al*. [1996]. The effects of land use are included by changing (decreasing with time) the total productive land area covered by the terrestrial biosphere. The carbon mass in each of the boxes is proportional to the total productive land area. Decreases in area lead to CO_2 emissions due to changes in land use as well as a decrease in the global rate of carbon exchange with the (smaller) biosphere. A simple model representation of biospheric feedbacks to changes in the atmospheric concentration of CO_2 and the global mean annual near-surface temperature are included. An increase in the rate of net photosynthesis (NP) of ground vegetation or net primary productivity (NPP) of trees by terrestrial biota, relative to preindustrial times, is modeled to be proportional to the logarithm of the relative increase in atmospheric CO_2 concentration from its preindustrial value. The magnitude of the mod-

eled biospheric sink depends primarily on the chosen value of the proportionality constant β known as the CO_2 fertilization factor [*Harvey*, 1989b; *Keeling*, 1973; *Wigley*, 1993]. In addition, the rate coefficients for exchange to and from terrestrial biosphere boxes (respiration and photosynthesis) vary with global mean annual temperature, which is calculated by an energy balance climate model [*Jain et al*., 1994] consistent with the model used by the Intergovernmental Panel on Climate Change (IPCC) [*Schimel et al*., 1996; *Watson et al*., 1990], according to a Q_{10} formulation, i.e., where net primary production and respiration rates are proportional to $(Q_{10})^{T/10°C}$, where T is the global-mean temperature, and Q_{10} is a model parameter [*Harvey*, 1989a]. The mechanism for biospheric feedbacks is not well characterized, leading to significant uncertainty in the prediction of the behavior of the future carbon cycle. The past net biospheric uptake, however, is constrained by the past carbon budget. We do not expect the past uptake of carbon isotopes to be highly sensitive to the mechanism for biospheric feedback, nor the split of the net biospheric uptake between emissions from changes in land use or biospheric feedback. If this expectation holds true for the modeled system, then isotopic data considered in section 5 will primarily constrain the net biospheric sink (and its location should spatially resolved data be used) and will have limited use in constraining the cause for changes in biospheric carbon.

The cycles of ^{13}C and ^{14}C are modeled by additional systems of equations of similar form as for total carbon, except for the inclusion of fractionation, radioactive decay of ^{14}C, and cosmogenic production of ^{14}C. A detailed description of the model equations for the atmosphere, ocean, and terrestrial reservoirs of CO_2 and its isotopes are given by *Jain et al*. [1995], *Kheshgi et al*. [1996], and *Jain et al*. [1996]. In this paper the ^{13}C concentrations are expressed as $\delta^{13}C$ [*Jain et al*., 1996], and ^{14}C concentrations are expressed here in the $\Delta^{14}C$ notation [*Jain et al*., 1995]. The model also takes into account the effects of radioactive decay. The radioactive decay constant for ^{14}C is $\lambda = 1.21 \times 10^{-4}\ \mathrm{yr}^{-1}$, whereas it is zero for the stable isotopes ^{12}C and ^{13}C.

3.2. Reconstruction of Anthropogenic Effects on the Past Carbon Budget

Estimates of the history of CO_2 emissions (measured in Gt C/yr) from the burning of fossil fuels $E_{\text{fossil fuel}}$ are greater than the sum of the modeled uptake of carbon by the oceans plus the observed accumulation of carbon (in the form of CO_2) in the atmosphere. In an attempt to balance the carbon budget we attribute the difference to the net uptake of carbon by the terrestrial biosphere [*Enting et al*., 1994; *Siegenthaler and Oeschger*, 1987; *Wigley*, 1993].

To reconstruct the past carbon budget, we calculate the history of land use emissions from

$$-\frac{dN_b}{dt} = \frac{dN_a}{dt} + \frac{dN_0}{dt} - E_{\text{fossil fuel}}. \tag{13}$$

$$\frac{dN_b}{dt} = S_{\text{biospheric feedbacks}} - E_{\text{land use}}. \tag{14}$$

The observed record of CO_2 concentration from the Siple ice core [*Friedli et al*., 1986], and from atmospheric measurements at the Mauna Loa Observatory in Hawaii [*Keeling et al*., 1995; *Neftel et al*., 1985], smoothed by a spline fit, is used to calculate the rate of change dN_a/dt of the carbon mass in the atmosphere. We adopt the estimate of the global emission rate $E_{\text{fossil fuel}}$ of CO_2 by the burning of fossil fuels given by *Marland et al*. [1994]. The ocean carbon cycle model [*Jain et al*., 1995] is used to calculate the rate of accumulation dN_0/dt of mass of carbon N_0 in the oceans with the atmospheric concentration of CO_2 specified to be the spline fit to the observed record. The net uptake of carbon by the terrestrial biosphere dN_b/dt is calculated from (13). To match the estimate of land use emissions of 11 Gt C [*Schimel et al*., 1996] for the decade of the 1980s, we calibrate the CO_2 fertilization factor β to equal 0.39. Land use emissions are then calculated from the rate of uptake of carbon by terrestrial biosphere feedbacks $S_{\text{biospheric feedback}}$, calculated in response to the spline fit to the observed history of atmospheric CO_2 [*Kheshgi et al*., 1996], and dN_b/dt by (14). In this way the modeled carbon cycle is forced to replicate the smoothed history of atmospheric CO_2 concentration. A similar approach was used by the IPCC [*Schimel et al*., 1996] to reconstruct the past carbon budget.

The past reconstruction of the ^{13}C and ^{14}C cycles are created on the basis of the reconstruction for total carbon as done by *Jain et al*. [1996]. We start from a model steady state. The ^{13}C steady state is determined by the fractionation of ^{13}C relative to ^{12}C and the exchanges of total carbon. The radiocarbon steady state adds the effects of a cosmic radiation source of radiocarbon in the atmosphere and decay of radiocarbon in all the carbon reservoirs. The model reconstruction departs from steady state driven by changes in fossil fuel, land use, and bomb-produced radiocarbon sources. The model reconstruction is determined, in part, by the set of model parameters discussed in the following section.

3.3. Parameterized Degrees of Freedom for Modeling Past Carbon Budget

A fundamental assumption in this use of Bayesian parameter estimation is that the parametric model contains sufficient degrees of freedom to approximate the behavior of past carbon cycle, so the error given in (1) is predominantly due to data errors and not the ability of the model to reproduce the data. Degrees of freedom should be included where there are weaknesses in our understanding of carbon cycle. Excessive degrees of freedom, however, will lead to an overestimate of uncertainty of the carbon budget. These degrees of freedom are represented in this analysis by the choice of parametric model for carbon cycle and the choice of prior parameter estimates.

The terrestrial carbon cycle model contains feedbacks driven by both CO_2 concentration and global temperature change, which allows a wide range of carbon source/sink rate. Fractionation factors common to all photosynthetic fixation of carbon in the model are used independent of, for example, the plants responsible. Detailed regional studies have used prescribed dependence of fractionation factor on water availability and plant type in their analysis [e.g., *Ciais et al*., 1995]. We have not included ranges of possible behaviors of fractionation factors, and this may unduly alter the effects of isotopic constraints on terrestrial carbon cycle. Reliable globally aggregated data on terrestrial carbon isotopic content are lacking [*Harrison et al*., 1993] and therefore have not been included in this study; this makes it difficult to evaluate the potential effect of this degree of freedom.

While ocean carbon cycle models that have been used to reconstruct the global carbon budget [*Enting et al*., 1994; *Jain et al*., 1995] exhibit various degrees of resolution, from a few carbon reservoirs to three-dimensional general circulation models, most models include air/sea exchange and tracer trans-

port (convection and diffusion) modified by biologically caused particulate transport. The relation between deep sea tracers and ocean carbon uptake differs between models with different convection schemes, and these differences cannot be represented by the two parameters, upwelling velocity w and diffusion coefficient k, conventionally used in an upwelling diffusion model [*Jain et al*., 1995]. In addition, ocean transport may not be time invariant as is often assumed, contributing to additional differences between modeled deep ocean tracers and carbon uptake. Both of these are potential contributors to uncertainty in modeled ocean carbon uptake to be considered. Neither is captured in the time-invariant transport parameters for upwelling or diffusion used in this model. We use the ocean bottom-water parameter π_c as a device to add a degree of freedom to account the effects of these two considerations on uncertainty estimates.

The bottom-water formation in the higher-latitude belts is quite well known [*Broecker and Peng*, 1982]. In this model, the downwelling flow in a polar sea zone represents the bottom-water-forming regions of the world oceans. This leads to a path for recently absorbed atmospheric CO_2 to reach the deep ocean. Rapid vertical exchange between the polar surface waters and the deep ocean has been considered in modeling the carbon cycle [*Siegenthaler*, 1983]. Tracers in high-latitude waters have been used to calibrate exchange coefficients with high-latitude waters in other model studies [*Kheshgi et al*., 1991; *Shaffer and Sarmiento*, 1995]. In this model, bottom-water concentration is controlled by a bottom-water parameter π_c, which is the ratio of the change in concentration of bottom-water N_b from its initial (1765) value N_{b0} to the change in concentration of the mixed layer N_m from its initial (1765) value N_{m0}:

$$\pi_c = \frac{N_b - N_{b0}}{N_m - N_{m0}}. \tag{15}$$

A value of $\pi_c = 1$ implies that the change in bottom-water concentration is the same as the change in mixed layer concentration. Note that the ratio of $^{14}C/^{12}C$ (or other preanthropogenic tracers) in the deep sea is insensitive to the value of π_c, since π_c does not affect the initial concentration of ^{14}C which dominates the current deep sea concentration. This insensitivity limits the extent to which π_c can be calibrated by tracers indicating the preanthropogenic state, which is assumed to be steady in this reconstruction. The use of this parameter therefore is to add a degree of freedom to the model which allows transport of surface water carbon to the deep sea independent of the initial concentration. Uncertainty in this parameter is used as a device to represent the effects of differing model structure on the relation of deep sea tracers to ocean uptake, and the effects of time-varying transport (transport not fully constrained by the preanthropogenic state) on the estimation of the past carbon budget.

Note that if the convection/diffusion field of ocean carbon cycle models are time invariant, then the globally aggregated carbon and isotope uptake of these models can be approximated by a single (Green's) function notwithstanding the spatial resolution of the model [*Kheshgi and White*, 1996; *Joos et al*., 1996]. An alternative to the ocean carbon cycle model used in this study could be the calibration of the Green's function subject to prior information which could be generated by more complex (e.g., three dimensional) but cumbersome models, although the characterization of time-varying convection would remain an obstacle.

4. Prior Estimates of Global Carbon Cycle Model Parameters

In this section we describe our choice of the base-case set of model parameters and the prior estimate of their probability distribution. We assume that the prior estimates are not correlated. The prior distribution of a parameter can therefore be characterized by its mean value and its standard deviation (or 90% confidence limit which is equal to 1.65 times the standard deviation); values are summarized in Table 1 with a detailed discussion in Appendix A.

Of the model parameters listed in Table 1 some are based on independent studies which prescribe an uncertainty, while others are not well known and will be better determined by Bayesian parameter estimation. For well-known parameters the mean values and standard deviation have been estimated in other studies from data independent from the data-based constraints that will be applied using Bayesian parameter estimation; for these parameters we adopt the estimates of their distributions. An example of a parameter well characterized by independent data is the history of fossil fuel emissions. Other model parameters are not easily measured, and their values have often been characterized using constraints. For these model parameters we choose a mean value that is consistent with the model calibration (see section 3.2) carried out by *Jain et al*. [1996] but specify a large standard deviation. By doing so we can assess the sensitivity to model parameters at their mean values which will give a fair representation of the model sensitivity over the constrained range of model parameters; by choosing a large standard deviation for these parameters we will not bias results with prior information, which has little basis beyond the constraints, which we will specify in section 5.

5. Definition of Constraints on Global Carbon Cycle

In this study we explicitly apply an extensive set of data-based constraints, summarized in Table 2 and discussed in detail in Appendix B, on the parametric model of the global carbon cycle. We consider only globally and annually aggregated (note that our carbon cycle model does not simulate seasonal variations) constraints, consistent with our model formulation. Spatial distributions of tracers could further constrain more detailed models of the global carbon cycle, but the extent to which the constraints can be strengthened has not been examined.

We have selected the discrete set of constraints and their data-based values given in Table 2 with consideration of the ill-defined characteristics of the data. Since the errors of the data-based estimates from the true values are assumed not to be correlated to each other, our selection does not include constraints that are expected to be correlated; for example, we do not include both the ocean inventory and the penetration depth of bomb-produced radiocarbon in the oceans, since these are based on some of the same sets of data and would introduce little additional information. Nor do we include time series data that may have correlated errors. The assumed Gaussian probability distributions of the constraints are characterized by their mean and variance which are chosen considering the previous studies that have made observation-based estimates along with the way in which we use the estimates as constraints. While the definition of constraints is subjective, the constraints are related to observation-based studies; fur-

Table 2. Data-Based Constraints and Uncertainties Described in Section 5 Compared to Model Output Generated Using the Mean Prior Estimate of Model Parameters and the Posterior Estimate of Model Parameters Given in Table 1

Model Output/Data Description*	Model Output for Mean Prior Estimate of Model Parameters	Data Constraint Mean Value ± 90% Confidence Interval	Model Output for Posterior Estimate of Model Parameters Mean Value ± 90% Confidence Interval
1. Atmospheric CO_2 accumulation (1765–1980)	126.1 Gt C	126 ± 11 Gt C	124.05 ± 9.37 Gt C
2. Atmospheric CO_2 accumulation (1980–1990)	33.0 Gt C	33 ± 4 Gt C	33.72 ± 3.65 Gt C
3. Atmospheric CO_2 (1990)	354.5 ppm	354 ± 2 ppm	353.99 ± 1.97 ppm
4. Average ocean total carbon (1975)	2.355 gC/m^3	2.33 ± 0.05 gC/m^3	2.33 ± 0.05 gC/m^3
5. Temperature change (1860–1990)	0.53°C	0.45 ± 0.15°C	0.45 ± 0.15°C
6. Atmospheric $\delta^{13}C$ (1956)	−7.04‰	−6.79 ± 0.17‰	−6.93 ± 0.08‰
7. Atmospheric $\delta^{13}C$ (1990)	−7.978‰	−7.90 ± 0.17‰	−7.86 ± 0.13‰
8. Atmospheric $\delta^{13}C$ change (1800–1953)	−0.586‰	−0.44 ± 0.23‰	−0.49 ± 0.07‰
9. Atmospheric $\delta^{13}C$ change (1978–1990)	−0.352‰	−0.40 ± 0.17‰	−0.34 ± 0.07‰
10. Surface ocean $\delta^{13}C$ (1975)	1.88‰	2.0 ± 0.17‰	2.01 ± 0.12‰
11. Surface ocean $\delta^{13}C$ change (1970–1990)	−0.352‰	−0.40 ± 0.23‰	−0.32 ± 0.07‰
12. Surface ocean $\delta^{13}C$ change (1800–1970)	−0.522‰	−0.5 ± 0.5‰	−0.41 ± 0.10‰
13. Ocean $\delta^{13}C$ inventory change (1970–1990)	−151.6‰ m	−208 ± 103‰ m	−150.68 ± 33.53‰ m
14. Atmospheric $\Delta^{14}C$ change (1860–1950)	−20.1‰	−20 ± 8‰	−20.28 ± 7.97‰
15. Surface ocean $\Delta^{14}C$ change (1900–1950)	−5.60‰	−12 ± 13‰	−5.99 ± 1.24‰
16. Surface ocean $\Delta^{14}C$ (1975)	111.8‰	110 ± 18‰	110.14 ± 17.68‰
17. Bomb-^{14}C ocean inventory change (1950–1975)	3.27×10^{28} atoms	$3.05 \pm 0.5 \times 10^{28}$ atoms	$3.12 \pm 0.33 \times 10^{28}$ atoms
18. Average ocean $\Delta^{14}C$ concentration (1975)	−158.5‰	−160 ± 8‰	−160.13 ± 7.95‰
19. ^{14}C ocean + biosphere inventory change (1965–1990)	3.51×10^{28} atoms	$3.2 \pm 0.4 \times 10^{28}$ atoms	$3.19 \pm 0.38 \times 10^{28}$ atoms

*All ranges of years listed are defined to be at their beginning (i.e., January 1).

thermore, the sensitivity of our final results to the choices made is studied explicitly.

6. Results of Bayesian Estimation of the Global Carbon Budget

6.1. Application of the Base-Case Set of Constraints and Prior Information

We apply Bayesian parameter estimation to arrive at posterior estimates of model parameters, and model outputs characterized by their mean values $\alpha_{\text{posterior}}$ and $M(\alpha_{\text{posterior}})$, and the covariance matrices $C_{\text{posterior}}$ and C_{output}. When we apply the full set of constraints listed in Table 2, we arrive at the posterior estimate (listed in Table 1) of model parameters with narrower distributions than the priors shown in Table 1. Comparison to the prior estimates in Table 1 shows that the confidence interval of some of the parameters has decreased significantly in size, whereas others have remained nearly unchanged: according to (10) the confidence interval of the posterior estimate must be narrower than that of the prior. For instance, the confidence interval for ocean upwelling velocity and vertical diffusivity decrease considerably due, in part, to the constraint on average ocean $\Delta^{14}C$ concentration; whereas the intervals for the climate effects of the terrestrial biosphere (the Q_{10} factors) are not affected greatly because of the lack of information in the constraints specified in Table 2 that is pertinent to these parameters. Note that these are ranges of parameters for the linearized model (7) to which the constraints have been applied and not the full nonlinear model described in section 3.

Key degrees of freedom which affect the ocean uptake of carbon in this model are parameterized by the w, k, and π_c [*Jain et al*., 1995]. The components of the posterior covariance matrix $C_{\text{posterior}}$ give the correlation coefficients relating these three parameters:

$$\text{correlation coefficient}(w, k, \pi_c) = \begin{pmatrix} 1 & -0.69 & -0.66 \\ & 1 & 0.46 \\ & & 1 \end{pmatrix}, \tag{16}$$

which indicates a negative correlation between w and either k or π_c. This means, for example, that for values of w higher than its mean estimate (contained in $\alpha_{\text{posterior}}$), both k and π_c will be more likely to have a value lower than their mean estimate. These parameters are partially constrained by the average ocean $\Delta^{14}C$ concentration. Even with this constraint, however, the posterior estimate of upwelling velocity (0.25 ± 7.55 m/yr) has a much wider range of values than the range from zero to 4 m/yr that has been previously used [*Enting et al*., 1994; *Hoffert et al*., 1981; *Kheshgi et al*., 1991; *Shaffer and Sarmiento*, 1995; *Volk*, 1984; *Volk and Liu*, 1988]. However, in using posterior estimates of parameters, their covariance (off-diagonal elements of $C_{\text{posterior}}$) should, of course, not be neglected.

The set of constraints (Table 2) has little effect on the estimates of many of the parameters. This leads to little difference between the posterior and prior estimates of many of the parameters. For example, the estimate of fossil emissions (1980–1990) of 55.17 ± 4.72 Gt C is only slightly improved from the prior estimate of 55 ± 5 Gt C, implying that the data were not an effective constraint on the estimate of fossil fuel emissions. In another example the terrestrial net primary productivity (NPP) had a prior estimate of 62 ± 30 Gt C/yr and a posterior estimate of 57.79 ± 28.97 Gt C/yr. *Broecker and Peng* [1993] postulated that ^{13}C could form an effective constraint on the size of the terrestrial carbon exchange reservoir, if more accurate data-based estimates of changes in ^{13}C inventories could be made. The constraints that we have imposed did not reduce the range of the terrestrial NPP estimate, which is

Table 3. Posterior Estimate of Model Outputs of Ocean and Terrestrial Carbon Sources/Sinks Resulting From Different Sets of Constraints Compared to the Model Output for the Mean Prior Estimate of Parameters

	Model Output for Mean Prior Parameter Estimate	Model Output for Posterior Estimate of Model Parameters Mean Value ± 90% Confidence Interval			
		All Constraints	No ^{14}C Constraints	No ^{13}C Constraints	No ^{13}C or ^{14}C Constraints
Ocean CO_2 accumulation (1765–1980)	101.36	79.44 ± 44.64 Gt C	80.94 ± 58.00 Gt C	98.43 ± 65.22 Gt C	107.07 ± 97.12 Gt C
Ocean CO_2 accumulation (1980–1990)	19.84	17.05 ± 7.47 Gt C	17.24 ± 10.45 Gt C	19.30 ± 10.98 Gt C	20.94 ± 17.57 Gt C
Net biospheric source (1765–1980)	69.21	44.96 ± 50.63 Gt C	47.04 ± 61.97 Gt C	66.04 ± 70.75 Gt C	74.57 ± 100.21 Gt C
Net biospheric source (1980–1990)	−1.72	−4.41 ± 9.79 Gt C	−4.19 ± 12.04 Gt C	−2.31 ± 12.75 Gt C	−0.72 ± 18.46 Gt C

related to the turnover time for the model terrestrial biosphere reservoirs.

A posterior estimate of model outputs is calculated using (11). Table 2 lists the mean value and the confidence interval of the posterior estimate of the model outputs which can be compared to the data-based values also in the table. For all of the model outputs the confidence interval is smaller than that of the data-based constraint; this is a consequence of (10). Also, the distributions of model outputs overlap with, or are contained within, the distributions of the data-based values. The ability of the model to simulate the variety of constraints given in Table 2 has been used as evidence of our ability to reconstruct the global carbon budget [*Broecker et al*., 1995; *Jain et al*., 1996; *Kheshgi et al*., 1996; *Siegenthaler and Sarmiento*, 1993]. While many of the outputs exhibit a similar size confidence interval, for some the confidence interval is much smaller. For example, the posterior confidence interval for the surface ocean $\Delta^{14}C$ change from 1900 to 1950 is much smaller than that of the data constraint (output 15 in Table 2). This implies both that the best estimate of this quantity has a smaller range (−6 ± 1‰) than the data-based value (−12 ± 13‰), and that the data are not an effective constraint on other quantities; of course, this conclusion is subject to the assumptions implicit in this approach.

Estimates of the mean value and covariance matrix of model output for which there are not data-based constraints can also be calculated. In Table 3 the mean value and the confidence interval of the oceanic and net biospheric sinks of carbon for the decade of the 1980s and for the time period 1765–1980 are given and can be compared to various studies of uncertainty in the contemporary carbon budget. The confidence interval of the ocean sink for the 1980s applying all the constraints is 17 ± 7 Gt C, which is not significantly different than that stated in recent reviews [*Schimel et al*., 1995; *Siegenthaler and Sarmiento*, 1993] which give a nominal value with a 90% confidence interval of ocean carbon sink of 20 ± 8 Gt C for the 1980s. The estimate for the net biospheric source for the 1980s of −4 ± 10 Gt C (see Table 4) is roughly equal to the ocean accumulation (sink) plus atmospheric accumulation minus the fossil fuel emission assuming that the uncertainty of each are not correlated (implying that the errors sum geometrically); this compares to the value inferred from the recent IPCC assessment of −2 ± 10 Gt C [*Schimel et al*., 1996]. This implies also that the prior estimate of land use emissions does not significantly improve the estimate of the net biospheric source. Furthermore, since the net biospheric source is equal to land use emissions minus other biospheric sinks (CO_2 fertilization and climate effects in this model [cf. *Kheshgi et al*., 1996]) and since the variance of estimates of land use emissions and the net biospheric source are similar, then the estimate of other biospheric sinks (often called the missing sink) is correlated to the estimate of land use emissions as well as the net biospheric sink.

The parametric model used in this study is based on the linear response of the globally aggregated model shown in Figure 1 to changes in model parameters, about the mean prior estimate of the model parameters. While this model will be a close approximation to the nonlinear model in the neighborhood of the mean prior parameter values, the linear model will depart from results of the nonlinear model for parameter values much different from the mean prior values. As can be seen in Table 1, both the prior and the posterior estimates of the

Table 4. Variance (Standard Error Squared) of Estimates Decreases If the Prior Uncertainty of a Parameter is Decreased

	Relative Change in Variance of Estimates	
Determined Prior Parameter	1980s Ocean Sink	1980s Net Biospheric Source
22. Ocean parameter π_c	−0.868	−0.465
17. Upwelling velocity	−0.410	−0.233
18. Vertical diffusivity	−0.319	−0.192
24. Cosmogenic generation of ^{14}C	−0.248	−0.132
6. ^{14}C atmospheric inventory (1950–1965)	−0.163	−0.087
19. Ocean NPP	−0.133	−0.093

We examined the relative decrease in the posterior estimate of the variance of the 1980s ocean sink in the case where all constraints given in Table 2 are applied with the prior information given in Table 1, to the case where the prior confidence interval of one parameter is set to zero (= {variance with one parameter determined and the remaining priors as stated in Table 1}/{variance with priors in Table 1} − 1). All 26 parameters given in Table 1 are tested. Listed are the parameters which, when determined (i.e., the prior confidence interval set to zero), lead to the largest decrease in the variance of the 1980s ocean sink estimate.

Table 5. Posterior Estimates of Model Outputs of Ocean and Terrestrial Carbon Sources/Sinks Resulting the Case When All Constraints Are Applied and the Prior Estimate of Ocean Bottom-Water Parameter π_c Is Set to 0.5 Compared to Results With Base Case Priors (Table 3)

	Model Output for Posterior Estimate of Model Parameters Mean Value ± 90% Confidence Interval	
	$\pi_c = 0.5$	Base Case Priors
Ocean CO_2 accumulation (1765–1980)	92.28 ± 18.20 Gt C	79.44 ± 44.64 Gt C
Ocean CO_2 accumulation (1980–1990)	19.24 ± 2.72 Gt C	17.05 ± 7.47 Gt C
Net biospheric source (1765–1980)	56.89 ± 33.60 Gt C	44.96 ± 50.63 Gt C
Net biospheric source (1980–1990)	−2.31 ± 7.16 Gt C	−4.41 ± 9.79 Gt C

model parameters do depart far from the mean prior values. If the nonlinear model is run with the mean posterior estimate of the linear model parameters (all constraints imposed) given in Table 1, for example, the calculated 1990 atmospheric concentration of CO_2 is 351.93 ppm, which is remarkably close to the posterior estimate of the linear model of 353.99 ppm (Table 2), given the significant difference in model parameters between the mean posterior estimate and the mean prior estimate (about which the model was linearized). For this case, however, the 1980s ocean uptake calculated by the nonlinear model is 20 Gt C as opposed to 17 Gt C from the linear model (Table 3), which is well within the uncertainty of the estimates but, nonetheless, different; both results are near the 1980s ocean uptake of 20 Gt C (Table 3) calculated with the mean prior parameter values. In this study, constraints are applied, and the parameters of the linear model are estimated, not the parameters of the nonlinear model. For this reason it is not appropriate to use parameter estimates from the linear analysis as input to the nonlinear model. For the range of parameter values given in Table 1 the nonlinear model may well give wild results that would not be consistent with the constraints. It is clear from results thus far that a wide range of model behavior is needed to yield an uncertainty in the carbon budget comparable to expectations [e.g., *Schimel et al*., 1996]. To extend this analysis to a more detailed analysis using a full nonlinear model will require acceptance of that model behavior over a wide parametric range. Key processes and constraints indicated by this linear analysis may facilitate analysis of a nonlinear estimation problem.

The estimates of this study are the result of the explicit application of a Bayesian estimation framework. These results depend on subjective choice of model, priors, and constraints, as opposed to the subjective probability distributions of the components of the carbon budget reported in recent reviews [*Schimel et al*., 1995; *Siegenthaler and Sarmiento*, 1993]. The effect of these subjective choices on estimates can be evaluated using our framework, which is objective given the choice of model, priors, and constraints which are stated explicitly. Using this framework, the effect of more accurate constraints, which might come from emerging data or the neglect of constraints on estimates of the carbon budget, can be evaluated.

6.2. Sensitivity of Results to the Prior Distribution of Model Parameters

Posterior estimates of the ocean and biosphere carbon uptake are sensitive to the choice of prior distribution of model parameters. To test the effect of prior information for each parameter on the carbon budget, we compare the posterior estimate (with the base set of constraints applied) of the variance (standard error squared) of the ocean sink and the net terrestrial source for the decade of the 1980s when one of the 26 parameters listed in Table 1 is determined (standard error of the parameter set to zero). The variance with one parameter determined is always less than or equal to the variance for the base set of priors given in Table 1. Table 4 lists the relative change in ocean sink and the net terrestrial source variance for the parameters with the six largest effects on ocean sink variance. The largest effect is caused by the ocean bottom-water parameter π_c, which accounts for 87% of the variance in the 1980s ocean uptake and 47% of the variance in the 1980s net terrestrial source (confidence intervals given in Table 3). The next largest effects are caused by the prior uncertainty of upwelling velocity and the vertical ocean diffusivity.

The posterior estimate of the carbon budget, calculated when the ocean bottom-water parameter π_c is specified to be exactly 0.5 (prior estimate = 0.5 ± 0), is shown in Table 5 and has a much narrower probability distribution than the carbon budget shown in Table 3 for the base set of priors and constraints. The confidence interval of ocean uptake over both time intervals (1765–1980 and 1980–1990) decreases from the base case to a greater extent than that of the net biospheric source. In this case (Table 5) the uncertainty in fossil emissions and atmospheric accumulation contribute more to the posterior confidence interval of the net biospheric source than the uncertainty of the ocean uptake, due to the reduced interval size (associated with fixing π_c) of the posterior estimate of the ocean uptake relative to that of the atmospheric accumulation (Table 2) or fossil emissions (Table 1). While the mean values of the ocean sink and biospheric source of the carbon budget shown in Table 5 are similar to that of previous assessments [*Schimel et al*., 1996], the confidence intervals are much smaller.

Associated with determination of π_c, the posterior estimates of model parameters become more accurate. Uncertainty in ocean upwelling and diffusivity remain the leading remaining causes of uncertainty in ocean uptake although the magnitude of their uncertainty is reduced from that listed in Table 1. Ocean upwelling w and diffusivity k remain negatively correlated when π_c is determined; from the $C_{\text{posterior}}$ elements,

$$\text{cov}\,(w, k) = \begin{pmatrix} 11.88\ \text{m}^2/\text{yr}^2 & -1.36 \times 10^3\ \text{m}^3/\text{yr}^2 \\ & 0.45 \times 10^6\ \text{m}^4/\text{yr}^2 \end{pmatrix}, \qquad (17)$$

and the correlation coefficient between w and k is −0.59.

We conclude that estimates of the uncertainty of past ocean uptake are affected primarily by the lack of prior determina-

tion of the ocean bottom-water parameter π_c in our formulation of the parameter estimation problem. However, as noted in section 4 and Appendix A, further increase in the width of the prior confidence interval of π_c has a diminishing effect on posterior estimates. As discussed in section 3.3, our introduction of a π_c with a wide confidence interval adds a degree of freedom to the system which decouples the relation between model parameters (and thus the modeled carbon budget) and constraints to the initial (1765) ocean steady state. Therefore while average ocean radiocarbon forms a constraint on w and k, it does not form a strong constraint on π_c. An effect of this degree of freedom is to avoid the constraints implicit in the model structure (time-invariant ocean transport and approximate deep ocean transport) which would otherwise highly constrain contemporary ocean uptake of carbon with data from deep ocean tracers. For comparisons shown in the remainder of this paper we shall use the base set of prior information listed in Table 1.

The use of π_c is an important point of departure from other studies of model calibration and uncertainty. For example, *Enting and Pearman* [1987] used the method of constrained inversion, a method related to Bayesian parameter estimation, to calibrate a carbon cycle model although they did not report the uncertainty of their posterior parameter estimates. In their analysis, data constraints were stated with larger uncertainties than used here (e.g., the specified standard error of their deep ocean $\Delta^{14}C$ constraint was $\pm 50‰$ compared with our $\pm 5‰$), and a small uncertain time gradient in ocean vertical diffusion was allowed in their prior distribution of model parameters; this yielded a comparable range of uncertainty as in this study but by a different path. Alternatively, *Heimann and Maier-Reimer* [1996] used air/sea balances as partial carbon cycle models, avoiding issues of deep sea transport; however, their analysis resulted in larger estimates of uncertainty than found here, which is due, in part, to consideration of a subset of the constraints included in Table 2, as is discussed in detail in section 6.3.

6.3. Effectiveness of ^{13}C Versus ^{14}C Constraints on the Carbon Budget

Subsets of the constraints listed in Table 1 lead to wider distributions of posterior estimates in model parameters as well as model outputs. Table 3 shows the model estimate of the reconstructed carbon budget for four sets of constraints. The first set of constraints (discussed above) is the application of all constraints listed in Table 2. The second is the result of neglecting all ^{14}C constraints (constraints 14–19 in Table 2). The third is the result of neglecting all ^{13}C constraints (constraints 6–13 in Table 2). The fourth is the result of neglecting all ^{13}C and ^{14}C constraints (constraints 6–19 in Table 2).

When isotopic constraints are not imposed, the probability distributions of ocean and biospheric uptake are considerably wider than the case where all isotopic constraints are imposed. This gives one set of measures of the degrees of freedom allowed by the model structure, prior estimates of parameters, and the remaining constraints. The wide range is caused in part by the wide range chosen for some of the model parameter priors, such as the fertilization factor (β), ocean upwelling velocity, ocean vertical diffusivity, bottom-water π_c, and ocean net primary production.

The effect of either ^{13}C or ^{14}C constraints is to narrow the uncertainty of the budget from that with no isotopic constraints. As can be seen in Table 3, ^{13}C constraints reduce uncertainty slightly more than ^{14}C constraints. Together, ^{13}C and ^{14}C constraints reduce uncertainty even further. An implication of this result is that globally aggregated ocean models calibrated with the radiocarbon [see *Jain et al*., 1995; *Siegenthaler and Joos*, 1992] miss the possibly stronger constraining effects of ^{13}C (whether this is also the case with spatially resolved data remains to be shown).

Heimann and Maier-Reimer [1996] compared the effects of various constraints implied by ^{13}C data on the 1980s carbon budget. In an attempt to make their evaluation of data constraints on the carbon budget model-independent, they applied globally aggregated mass balances as their model and then performed the equivalent of a Bayesian parameter estimation. In order to see if the results of our analysis are comparable to those of *Heimann and Maier-Reimer* [1996], we choose a subset of the constraints in Table 2 to enforce the primary constraints in the *Heimann and Maier-Reimer* [1996] analysis: all the nonisotopic constraints (1–5 in Table 2) along with a subset of the ^{13}C constraints (7–11 and 13 in Table 2). Application of this set of constraints leads to an estimate of 1980s ocean sink of 21.7 ± 11.3 Gt C using our framework. Whereas *Heimann and Maier-Reimer*'s [1996] combined the three ^{13}C balances, they considered and arrived at an estimate of 1980s ocean sink of 21 ± 15 Gt C (90% confidence interval). We do not directly reproduce the budgets as stated by *Heimann and Maier-Reimer* [1996], because the definitions of our constraints and our model, which simultaneously accounts for all the balances, differ from those of *Heimann and Maier-Reimer* [1996] whose results show a wider confidence interval. Of course, application of both ^{13}C and ^{14}C constraints yields a much narrower distribution.

6.4. Strength of Individual Constraints on the Carbon Budget

To test the effect of each constraint on the carbon budget, we compare estimates of the variance (standard error squared) of the ocean sink for the decade of the 1980s when (1) all but one constraint is applied and (2) the uncertainty of one constraint is reduced by half. Table 6 shows the increase in the variance estimate, relative to that for the case when all constraints in Table 2 are applied, for the constraints with the six largest effects. Average ocean $\Delta^{14}C$ concentration in 1975 is the constraint with the largest effect on estimated variance of the ocean sink.

Omission of many individual constraints had only a minor effect on posterior estimates. For example, the constraint (constraint 19) on the atmospheric inventory plus bomb production of radiocarbon over the period from 1965 to 1990 had very little effect; omitting this constraint increased the 1980s ocean sink variability by 0.007 (relative, compare Table 6), which was the 15th largest effect of the 19 constraints. This is consistent with our previous conclusion [*Jain et al*., 1997] that the uncertainty of the data-based estimate of this quantity was too great to make this an effective constraint on global carbon budget.

Average ocean radiocarbon concentration limits the turnover time for the deep sea, which is parameterized in the model by ocean transport parameters: upwelling velocity and diffusivity. Note that the average ocean $\Delta^{14}C$ is primarily a measure of the preanthropogenic deep sea $\Delta^{14}C$ which is not affected by π_c in the model, as is evident in (15).

Strengthening of constraints (i.e., reduction of the uncertainty of on one of the data-based constraints) reduces the variance of the ocean sink estimate somewhat. The ordering of

Table 6. Variance (Standard Error Squared) of Estimates Increases If the Number of Constraints Applied Is Reduced, and the Variance Decreases If Any of the Constraints Are Strengthened

Constraint	Relative Change in Variance of 1980s Ocean Sink Estimate	
	Omission of One Constraint	Uncertainty of One Constraint Halved
18. Average ocean $\Delta^{14}C$ concentration (1975)	0.337	−0.070
16. Surface ocean $\Delta^{14}C$ (1975)	0.226	−0.006
7. Atmospheric $\delta^{13}C$ (1990)	0.130	−0.079
17. Bomb-^{14}C ocean inventory change (1950–1975)	0.094	−0.152
13. Ocean $\delta^{13}C$ inventory change (1970–1990)	0.075	−0.026
14. Atmospheric $\Delta^{14}C$ change (1860–1950)	0.067	−0.0004

We examine the change in the variance of the 1980s ocean sink, from the case where all constraints are applied, to the cases where one constraint is altered (= {variance with one constraint altered}/{variance with all constraints} − 1). In one set of results the altered constraint was removed (i.e., all but one constraint is applied), whereas in the second set of results, the uncertainty of the altered data-based constraint is reduced by a factor of 2 (i.e., one constraint is strengthened). All 19 constraints listed in Table 2 were tested. Listed are the constraints which when omitted lead to the largest increase in variance.

the constraints with the largest effect is different in this test (see Table 6) than in the test where a constraint is omitted. The largest effect is seen by reducing the uncertainty in the change in bomb-radiocarbon inventory (constraint 17), as opposed to the average ocean $\Delta^{14}C$ (constraint 18) which had the largest effect when omitted. However, reducing the uncertainty in this constraint by a factor of 2 results in a reduction of the 1980s ocean sink variance by only 15%.

Omitting or strengthening constraints has a similar effect on uncertainty estimates of the terrestrial biospheric source as on ocean uptake. Omitting the average ocean $\Delta^{14}C$ (constraint 18) leads to the largest increase in the variance of the estimated 1980s terrestrial biospheric source, as with the 1980s ocean uptake. The largest effect of strengthening a constraint on the 1980s terrestrial biospheric source is found by reducing the uncertainty in the change in bomb-radiocarbon inventory (constraint 17), as with the 1980s ocean uptake; however, reducing the uncertainty in this constraint by a factor of 2 results in a reduction of the 1980s terrestrial biospheric source variance by only 10%.

7. Concluding Discussion

We have estimated the net uptake of carbon by the oceans and the terrestrial biosphere by using a globally aggregated model for carbon cycle along with carbon isotopic data which form constraints on the contemporary global carbon budget. By means of Bayesian parameter estimation we have made a quantitative reconstruction of the past carbon budget and characterized its uncertainty. Many studies have used subsets of carbon isotopic data to estimate the magnitude of ocean and terrestrial carbon sinks but often without a full characterization of the uncertainty of their estimates. In this study, model parameters and model outputs are characterized by their mean estimated value and covariance matrix. Our estimate, for example, of the ocean sink for the 1980s resulting from the application of the full set of constraints shown in Table 2 is 17 ± 7 Gt C (90% confidence interval), which is consistent with that stated in recent reviews [*Schimel et al*., 1995; *Siegenthaler and Sarmiento*, 1993]. It is important to note, however, that the wide range of model parameters that are required to arrive at this degree of uncertainty are not portrayed in projections of future growth of atmospheric CO_2 concentration [*Schimel et al*., 1995].

Estimates of the net uptake of carbon by the oceans and the terrestrial biosphere depend on prior estimates of model parameters. We see a large reduction of uncertainty in our estimate of ocean carbon uptake if we prescribe a narrow prior distribution of the ocean bottom-water parameter π_c, a parameter that allows transport of mixed layer carbon (and isotopes) to the deep sea without affecting the preanthropogenic concentration depth structure of our model ocean. We use this parameter as a device to represent potential uncertainty caused by assuming a model transport structure and time-invariant transport parameters. There are many other alternatives to the use of this specific device, and we recommend that these be considered, especially if estimating the uncertainty of projections of atmospheric response to future emissions. Nevertheless, we found a degree of freedom, such as that introduced by an uncertain π_c, is needed to arrive at an uncertainty in the carbon budget as large as that stated in recent reviews [*Schimel et al*., 1995; *Siegenthaler and Sarmiento*, 1993]. Without this degree of freedom we arrive at much more certain estimates of ocean and terrestrial carbon sinks; for example, the 1980s ocean sink is estimated to be 19 ± 3 Gt C (see Table 5).

The framework applied in this study allows evaluation of the effect of more accurate constraints that might come from emerging data or the neglect of constraints on estimates of the carbon budget. The effect of either ^{13}C or ^{14}C constraints is to narrow the uncertainty of the budget from that with no isotopic constraints. As can be seen in Table 3, ^{13}C constraints reduce uncertainty slightly more than ^{14}C constraints. Together, ^{13}C plus ^{14}C constraints reduce uncertainty even further. We find that omission of the average ocean $\Delta^{14}C$ concentration has the largest effect on our modeled carbon budget of the constraints that we have considered [cf. *Oeschger et al*., 1975]. This is the primary constraint on exchange between the deep ocean and the surface waters. While transient measures of ocean composition, such as bomb-^{14}C inventories, have been the focus of many recent analyses [cf. *Heimann and Maier-Reimer*, 1996; *Jain et al*., 1995, 1997], this globally aggregated study shows that neglect of any one of these constraints has but a small effect on the uncertainty of the ocean and terrestrial sinks

since other constraints contain closely related information making the constraints nearly redundant. However, if single constraints are strengthened, then the change in ocean bomb-^{14}C inventories has the largest effect on budget estimates.

There are several implications of this approach to estimating uncertainty. First, a single model can be devised which is consistent with the many carbon dioxide and isotopic constraints but yields a greater uncertainty than implied by comparisons of different model best guesses [cf. *Bruno and Joos*, 1997]. Second, the primary mode of uncertainty (or degree of freedom) for the ocean sink in this study is mechanisms that affect the relation between deep ocean tracers and transport between the ocean surface and deep waters. Finally, while the uncertainty of the ocean and terrestrial sinks are large, for example, for the recent decade (1980–1990), they are forced to cancel in order to balance the carbon budget. This effect results in correlation of posterior estimates of model parameters found in this study. While these uncertainties do cancel in the recent past, we expect that this will not be the case for projections of the distant future. In future projections, nonlinear and uncertain mechanisms could limit the effects of data-based constraints from the past; this will be the next step in our research.

One could go further with this approach by carrying out a full nonlinear analysis and using complex terrestrial biosphere and ocean carbon cycle models (e.g., three dimensional) which give detailed and realistic simulations of carbon cycle, once the degrees of freedom in these models have been characterized and represented by probability distributions of model parameters. This would, in theory, allow the use of spatially disaggregated data which would include more information. In this study we used a parametric carbon cycle model and found, however, that the parameter π_c was needed as a device to account for the anticipated effects of model structure uncertainty. With complex models the characterization of model structure uncertainty will need to be addressed as well and may negate some of the advantages that complex models provide.

8. Key Conclusions and Recommendations

1. The global records of carbon dioxide and carbon isotopic constraints considered in this study lead primarily to an estimate of ocean carbon uptake, which results in a terrestrial source or sink estimated as the residual of the carbon budget.

2. Our limited understanding of what controls exchange with deep ocean water is the key factor in estimates of the carbon budget in this study. In the global carbon cycle model shown in Figure 1, this process is represented by parameters for the carbon concentration of newly formed bottom water, upwelling, and diffusivity. These three parameters, in that order, are the primary factors determining the uncertainty of carbon budget estimates.

3. Leaving the parameter representing the carbon concentration of newly formed bottom water poorly determined led to an estimate of ocean carbon uptake comparable to its expected range. Fixing this parameter, as is implicitly done in many carbon cycle models, leads to an overconstraint of the estimation problem. Development of alternative model formulations, which better capture the effect of this model degree of freedom, is recommended.

4. A large uncertainty in model parameters is needed to represent our current expectation of the accuracy of the carbon budget.

5. ^{13}C records provide a slightly stronger constraint than ^{14}C records. The two sets of records, taken together, lead to a stronger constraint and a more certain carbon budget.

6. Omission of the average ocean Δ^{14}C constraint leads to the largest increase in estimated uncertainty of the carbon budget.

7. Decreasing the uncertainty of the global bomb-^{14}C inventory constraint leads to the largest decrease in estimated budget uncertainty. However, the improvement of the budget estimate is small for a significant decrease in constraint uncertainty.

8. Alternative constraints from other data records (e.g., O_2/N_2 records), or alternative priors from detailed process studies (which can make use of spatially resolved data) could be better paths to reductions in carbon budget uncertainty than efforts to further reduce uncertainty of data-based constraints used in this study. Such additional information could be included in a Bayesian estimation procedure as used here by inclusion of additional data constraints or by modification of priors.

9. Improvements in the estimation procedure used here could be made by consideration of alternative model structures, consideration of nonlinear parameter effects by using nonlinear estimation methods, and improved prior estimates based on physical considerations (e.g., nonnegative prior distributions of model parameters). Parameters and constraints found to be unimportant in this study could be used to simplify more detailed studies of the past carbon budget.

10. Factors that are not important in estimation of the past carbon budget can be important in estimates of the future carbon cycle response to emissions. For example, climate-sensitive processes (e.g., represented by Q_{10} factors in this study) will be important in the future if there is a substantial change in climate. This estimation procedure could be extended to look at the relation between past carbon budget and future estimates of carbon cycle.

Appendix A: Description of Prior Parameter Estimates

A1. Fossil Emission (1765–1980) and (1980–1990)

Values of fossil fuel emissions are taken from *Marland et al.* [1994]. The 90% confidence interval for the 1980s of $\pm 9\%$ is consistent with that of the recent IPCC assessment [*Schimel et al.*, 1996], and we choose a somewhat higher ($\pm 13\%$) interval for the 1765–1980 period to reflect greater uncertainty in fossil fuel use data over this period.

A2. Land Use Emission (1765–1980) and (1980–1990)

Values of land use emissions and its confidence interval for the 1980s are taken to be equal to the source due to tropical deforestation minus the sink due to Northern Hemisphere forest regrowth (errors assumed uncorrelated) assessed in the recent IPCC assessment [*Schimel et al.*, 1996]. Land use emissions for the 1765–1980 time period match those required for the model to reconstruct the atmospheric record of CO_2, as done by previous studies [*Jain et al.*, 1995; 1996; *Kheshgi et al.*, 1996], when evaluated with the mean prior values of the model parameters. The relative confidence interval for this period is taken to be slightly less than that for the 1980s because of the large reduction of temperate forests evident in historical records [*Schimel et al.*, 1995].

A3. Average Annual Fossil Fuel ^{13}C Content (1765–1990)

The time evolution of $\delta^{13}C$ in the atmosphere, oceans, and biosphere is calculated with the addition of information on the $\delta^{13}C$ history of fossil fuel emissions. For $\delta^{13}C$ of fossil fuel emissions from 1850 to 1950 we use the estimates given by *Tans* [1981a]. After 1950 we use the estimates given by *Andres et al*. [1995], which is based on updated fossil and cement production data [*Marland et al*., 1994]. The estimated value of $\delta^{13}C$ in 1990 is $-28‰$, which is $4‰$ less than the estimated 1850 value of $-24‰$. Prior to 1850 we assume that the $\delta^{13}C$ of fossil fuel emissions is equal to the 1850 estimate. We maintain the time profile of the $\delta^{13}C$ of fossil fuel emissions but allow for scaling of the entire series. We define this parameter as the average of the annual $\delta^{13}C$ values from 1765 to 1990 and assign a confidence interval of $\pm 9\%$ to this value.

A4. ^{14}C Atmospheric Inventory (1950–1965) and (1965–1990)

Prior to 1950 the time evolution of $\Delta^{14}C$ in the atmosphere, oceans, and biosphere is calculated. After 1950, aboveground testing of nuclear weapons led to a source of radiocarbon in the atmosphere. The rate of bomb production of radiocarbon, however, is not well known. In this study we prescribe the global-average observed atmospheric $\Delta^{14}C$ after 1950 [*Broecker and Peng*, 1994; *Tans*, 1981b], calculate the response of $\Delta^{14}C$ in the oceans and biosphere, and infer the bomb-^{14}C production rate from the rate of change of the changes in atmosphere/oceans/biosphere inventory of ^{14}C. To represent uncertainty in the prescribed time course of atmospheric ^{14}C inventory, we choose two time periods, one for the period of intense nuclear weapons testing and a correspondingly high ^{14}C source in the atmosphere (1950–1965) and the other showing a decrease in ^{14}C, and prescribe a confidence interval for each of $\pm 10\%$.

A5. Q_{10} Factors

These factors represent the temperature dependence of exchange coefficients to and from the reservoirs of the biosphere model. Their mean values were chosen to equal that prescribed in previous studies [*Harvey*, 1989a; *Kheshgi et al*., 1996], and the confidence interval of these parameters was chosen to represent the poor understanding of the past changes in these exchange rates.

A6. Fractionation Factor Atmosphere $\Rightarrow$ Ocean, Ocean $\Rightarrow$ Atmosphere, Atmosphere $\Rightarrow$ Terrestrial Biosphere, and Ocean $\Rightarrow$ Marine Biosphere

The ^{13}C fractionation coefficients (and standard errors) between the atmosphere and ocean are taken from *Siegenthaler and Münnich* [1981]. The ^{13}C fractionation coefficients for terrestrial and marine biospheres are taken from *Broecker and Peng* [1982] and *Keeling et al*. [1989], respectively. The ^{14}C fractionation coefficients for all processes are the square of those for ^{13}C [*Keeling*, 1981].

A7. Fertilization Factor

The specified mean prior value of $\beta = 0.39$ (along with the mean priors of the other parameters) leads to a reconstruction of the past carbon budget [*Jain et al*., 1996] which is consistent with a land use emission estimate of 11 Gt of carbon (Gt C) for the 1980s [*Schimel et al*., 1996]. The confidence intervals is chosen large enough to reflect the large uncertainty in estimates of the strength of this effect.

A8. Upwelling Velocity and Vertical Diffusivity

The mean values of these parameters were found by *Jain et al*. [1995] to match the global-average vertical profile of radiocarbon concentration which is related to constraints 16 and 18 listed in Table 2. The confidence intervals of both parameters is chosen large enough so that their prior information does not constrain the model carbon budget.

A9. Ocean NPP

A marine biosphere source term is included in the deep sea associated with the oxidation of the organic debris exported (net production) from the mixed layer where it is produced by photosynthesis [*Jain et al*., 1995; *Volk and Hoffert*, 1985]. In our model the surface ocean marine biogenic flux of carbon is 8.5 Gt C/yr which lies near the center of the observed range of 2–20 Gt C/yr [*Siegenthaler and Sarmiento*, 1993; *Sundquist*, 1985]. Again, the confidence interval is chosen large enough so that this prior information does not constrain the model carbon budget.

A10. Mixed Layer Depth

The mean prior value of mixed layer depth is identical to that used in prior studies [*Jain et al*., 1995, 1996]. The confidence interval of this parameter is chosen large enough to incorporate the range of depths used in other studies.

A11. Atmospheric Rate of Exchange, k_a

A global-mean gas-exchange rate at a preindustrial CO_2 concentration of 278 ppm of 17.0 mol/m^2/yr was estimated to satisfy the ^{14}C balance between the atmosphere and the ocean surface reservoirs for the steady state (1765) concentrations of radiocarbon given preindustrial expectations of concentrations of radiocarbon in the atmosphere and ocean mixed layer [*Jain et al*., 1995]. This value is slightly lower than 17.4 mol/m^2/yr adopted by *Hesshaimer et al*. [1994] or 17.8 mol/m^2/yr estimated by *Broecker and Peng* [1994], and higher than 16.6 mol/m^2/yr estimated by *Toggweiler et al*. [1989] or 15.2 mol/m^2/yr estimated by *Siegenthaler and Joos* [1992]. This value corresponds to an atmospheric rate of exchange of $k_a = 0.109\ \text{yr}^{-1}$ [*Jain et al*., 1995] for which we assign a standard error of 0.02 yr^{-1} which encompasses the different estimates of global-mean gas-exchange rate.

A12. Ocean π_c Parameter

This parameter represents the effect of mixed layer concentration on that of produced bottom water; see (15). The mean value is equal to that used by *Jain et al*. [1995], and the confidence interval is chosen large enough so that this prior information does not affect posterior estimates of the model carbon budget.

A13. Apparent Climate Sensitivity

Climate sensitivity relates changes in global-mean–annual temperature to changes in global forcing of climate for doubling of CO_2 concentration. In this study we use the sensitivity as a parameter to represent the range of past changes in the global-mean–annual temperature which form a constraint on this parameter.

A14. Cosmogenic Generation of ^{14}C

The changes in atmospheric ^{14}C are effected by changes in ^{14}C production rates which are correlated to the sunspot index [*Stuiver and Quay*, 1980]. While variations in the production

rate of ^{14}C are evident, these variations have a negligible effect on ^{14}C ratio [*Bacastow and Keeling*, 1973] over the timescale of 100 years (1850–1950); we do not therefore account for this effect in our calculations and thus assume a constant rate of cosmic ^{14}C production. The production rate does, however, determine the initial state of radiocarbon in our model system as described by *Jain et al*. [1995]. The mean production rate of ^{14}C from cosmic rays has been estimated to be 2 atoms/cm^2/s^1 [*Craig*, 1957; *Suess*, 1955]. More recently, *O'Brien* [1979] estimated cosmogenic production rate over the period 1937–1970 to vary between 1.88 and 2.12 atoms/cm^2/s, and *Stuiver and Quay* [1980] estimated the mean ^{14}C production rate from neutron flux and sunspot index measurements to be 1.88 ± 0.38 atoms/cm^2/s over the period from 1868 to 1967. However, when the sunspot index is assumed zero, the estimated mean ^{14}C production rates of *O'Brien* [1979] and *Stuiver and Quay* [1980] are both ~2.0 atoms/cm^2/s, consistent with the value used in this study. We choose a mean production rate of ^{14}C from cosmic rays to be 2.0 atoms/cm^2/s with a confidence interval of 0.5 atoms/cm^2/s.

A15. Terrestrial NPP (1765)

The net primary productivity of the terrestrial biosphere is adjusted in the model by scaling all exchange coefficients to and from the reservoirs of the biosphere. The mean prior value is identical to that of previous studies [*Harvey*, 1989a; *Kheshgi et al*., 1996]. The variance of estimates of current terrestrial NPP [*Schlesinger*, 1991] indicates the level of uncertainty in estimates of NPP.

A16. Atmospheric pCO_2 (1765)

The initial atmospheric pCO_2, assumed to be at steady state, is taken from the Siple ice core [*Friedli et al*., 1986; *Neftel et al*., 1985] with the confidence interval estimated from the variance of ice core data.

Appendix B: Description of Data-Based Constraints

B1. Atmospheric CO_2 Concentration

In the initial calibration of the model, as discussed in section 3.2, an inverse model calculation is run with the time history of atmospheric CO_2 specified and the time history of land use emissions calculated. Thereafter, the model is run as a forward calculation, so as parameters are varied, the modeled atmospheric concentration will deviate from the observed values. In addition, estimates of land use emissions are used (see section 4) to modulate the amplitude of the land use emission time series found by inverse model calculation. We characterize the time history of atmospheric CO_2 by the atmospheric concentration (annually averaged) at the beginning of 1990 along with the change in atmospheric content over two time periods: 1765 to the beginning of 1980 and 1980 to 1990 (the decade of the 1980s). The uncertainty that we prescribe for these constraints stems from the uncertainty that the estimate represents the true global mean-annual CO_2 concentration of the atmosphere and the natural variability (e.g., interannual variability of the global mean) that the CO_2 concentration exhibits (which our parametric model has not been designed to simulate).

An estimate of atmospheric accumulation of CO_2 from 1765 to 1980 of 126 Gt C [*Kheshgi et al*., 1996] is calculated from the changes in atmospheric CO_2 concentration measured from the Siple ice core [*Friedli et al*., 1986] and at the Mauna Loa Observatory [*Keeling et al*., 1989; *Keeling and Whorf*, 1993]. The uncertainty of this estimate is dominated by the uncertainty of the estimate of the 1765 concentration of CO_2 of 280 ppm which we take to have a 90% confidence interval (= 1.65 times the standard error) of 5 ppm (11 Gt C) based on the variability of ice core records of CO_2 concentration.

An estimate of atmospheric accumulation of CO_2 from 1980 to 1990 of 32 Gt C was given in the IPCC 1994 special report [*Schimel et al*., 1995] along with an uncertainty estimate of 2 Gt C (90% confidence interval) presumably based on atmospheric sampling error. This estimate was revised in the IPCC Second Assessment Report to 33 Gt C with the same uncertainty estimate [*Schimel et al*., 1996]. In this study we add to the uncertainty the expected size of anomalies in the atmospheric content which we take to have a standard deviation of ~1 ppm which then corresponds to a standard error of 2 Gt C. The assumption that these two sources of error are uncorrelated leads to a total uncertainty of 4 Gt C (90% confidence interval). Note that the anomalies are a larger source of uncertainty than our ability to measure the global-mean atmospheric concentration.

An estimate of the seasonally smoothed atmospheric concentration of CO_2 at the end of 1989 of 354 ppm is inferred from data from the Mauna Loa Observatory [*Keeling and Whorf*, 1993]. The uncertainty is taken to be the same as for the 1980s interval of 2 ppm (90% confidence interval).

B2. Average Ocean Total Inorganic Carbon Concentration

The deep ocean average dissolved inorganic carbon at the time of the GEOSECS survey was estimated by *Hoffert et al*. [1981] to be 2.33 gC/m^3 for use in constructing an upwelling diffusion model of the oceans. Alternatively, *Takahashi et al*. [1981] estimated a slightly lower value (2.31 gC/m^3) from GEOSECS data. We adopt a value of 2.33 gC/m^3 with a standard error of 0.03 gC/m^3.

B3. Global Temperature Change

In our modeled reconstruction of carbon cycle, changes in temperature are taken to affect the rate coefficients between reservoirs of the terrestrial biosphere model as well as the partial pressure of carbon dioxide of seawater. We specify the observed trend of global near-surface temperature change from 1860 to 1990 of 0.45°C in order to constrain the range of temperature change over the period of our reconstruction. The 90% confidence interval of 0.15°C is taken to reflect the IPCC assessment [*Schimel et al*., 1996] that there has been a global increase in temperature from 0.3°C to 0.6°C since the late 19th century.

B4. Atmospheric $\delta^{13}C$

Friedli et al. [1986] measured the atmospheric $\delta^{13}C$ of CO_2 from the ice core taken at Siple Station in Antarctica from 1765 to 1953. The ice core measured values in ~1800 and in 1953 were −6.41 and −6.85‰ [*Friedli et al*., 1986]. Accuracy of the $\delta^{13}C$ ice core measurements is ±0.10‰, as determined by analyzing artificial CO_2 in air-mixtures and from the scatter of the Siple results around the smooth line. We adopt an overall change from 1800 to 1953 of −0.44‰ with an estimated standard error of ±0.14‰.

Atmospheric $\delta^{13}C$ is also measured directly at the Mauna Loa Observatory and a continuous record extends back to 1978. Prior to 1978 a measurement of −6.79‰ from the Mauna Loa Observatory is available for the year 1956 [*Keeling et al*., 1979]. Recent Mauna Loa data for 1990 show a $\delta^{13}C$ of

−7.90‰ and a change from 1978 to 1990 of 0.40‰. The uncertainty in approximating the globally averaged value with the Mauna Loa data has been estimated to have a standard error of ±0.024‰ [*Keeling et al*., 1995]. However, there is considerable interannual variability that led *Heimann and Maier-Reimer* [1996] to use a standard error of 0.1‰ for the atmospheric ratio and standard error of 50% for the recent trend. We adopt an atmospheric $\delta^{13}C$ for 1956 of −6.79 ± 0.1‰, a change from 1978 to 1990 of −0.40 ± 0.1‰, and for 1990 of −7.90 ± 0.1‰ (standard error).

B5. Surface Ocean $\delta^{13}C$

Ocean surface water $\delta^{13}C$ from recent to preindustrial (~1800) times is available from analyses of local coral and sclerosponge. Results of ^{13}C analyses were reported by *Nozaki et al*. [1978] of a Bermuda coral and *Druffel and Benavides* [1986] of a Jamaican sclerosponge. The Nozaki et al. study indicates a $\delta^{13}C$ change of −0.46‰ in the ocean surface water over the period 1800–1970 with a standard error of 0.10‰. *Druffel and Benavides* [1986] measured the change of −0.5‰ from 1800 to 1972 with a standard error of ±0.07‰. We adopt the constraint of $\delta^{13}C$ mixed layer change from 1800 to 1970 of −0.5‰ ± 0.3‰; the high standard error accounts for the poor of spatial coverage and the high spatial variability evident in GEOSECS data for the Atlantic [*Tans et al*., 1993].

An estimate based primarily on GEOSECS data showed that the average surface water $\delta^{13}C$ was ~2.0‰, but local values were highly variable due to biological and air-sea mixing processes [*Kroopnic*, 1985; *Tans et al*., 1993]. *Kroopnic* [1985] estimated the uncertainty of this average to be ±0.10‰ [*Kroopnic*, 1985]. As one constraint on surface $\delta^{13}C$, we adopt a 1974 value of 2.0 ± 0.10‰ (standard error). Note that this value combined with an atmospheric $\delta^{13}C$ give an implied constraint on air/sea disequilibrium which was used in earlier studies [*Heimann and Maier-Reimer*, 1996; *Tans et al*., 1993].

Quay et al. [1992] used additional data to estimate a change in $\delta^{13}C$ of −0.4‰ from 1970 to 1990 in the mixed layer of the Pacific Ocean and assigned an uncertainty of ±0.04‰ to this estimate. This uncertainty is significantly smaller than either of the above estimates for the GEOSECS global average. We adopt a the constraint of $\delta^{13}C$ mixed layer change from 1970 to 1990 of −0.4‰ ± 0.14‰ (standard error assuming an uncorrelated standard error of ±0.1‰ at each end of the time range).

B6. Ocean $\delta^{13}C$ Inventory

Quay et al. [1992] estimated the change in the depth-integrated $\delta^{13}C$ and penetration depth between 1970 and 1990 based on $\delta^{13}C$ measurements in the Pacific Ocean and the ocean-wide extrapolation with the use of the bomb-^{14}C distribution. Since penetration depth and inventory are correlated, we choose to include only the inventory. The *Quay et al*. [1992] estimate of inventory of −208 ± 45‰ m was reconsidered by *Heimann and Maier-Reimer* [1996], who explained that the standard error of ±45‰ m did not include all sources of uncertainty and made a new estimate of a standard error of 62‰ m which we adopt.

B7. Atmospheric $\Delta^{14}C$

Stuiver and Quay [1981] measured, with high precision, tree-ring ^{14}C in the state of Washington. They found a reduction in $\Delta^{14}C$ of −20 ± 1.2‰ between 1860 and 1950. However, *Tans* [1978] measured the decrease of $\Delta^{14}C$ for trees grown in Europe of −25‰. We adopt a change in atmospheric $\Delta^{14}C$ of −20 ± 5‰ (standard error) over the period 1860–1950.

B8. Surface Ocean $\Delta^{14}C$

The decline of surface ocean $\Delta^{14}C$ recorded by corals varies from location to location. Florida coral recorded a change of −11‰ from 1900 to 1952 [*Druffel and Linick*, 1978]. Belize coral showed a change of −12‰ during this period [*Druffel*, 1980]. Galapagos coral showed the smallest change of −6‰, and the Bermuda coral showed the largest change of −20‰ in $\Delta^{14}C$ of the ocean surface layer over the same time period [*Druffel*, 1981]. We use a surface ocean $\Delta^{14}C$ change of −12‰ over the period 1900–1950 based on the average of Florida, Belize, Galapagos, and Bermuda corals and assign a standard error of ±8‰.

Coral data also show a large rise of surface ocean $\Delta^{14}C$ concentration from about 1954 to 1975, which we attribute to the net transfer of bomb-produced ^{14}C from the atmosphere to the surface ocean. Radiocarbon in both Florida and Belize coral show an overall increase over the period 1954–1975 of 214‰ presumably due to the increase of bomb-produced ^{14}C in the surface waters of the Gulf System. *Broecker et al*. [1985] estimated the mean surface ocean $\Delta^{14}C$ increase of 155‰ over the period 1955–1975. Their value of 155‰ is based on the prebomb surface water samples [*Broecker*, 1985] and GEOSECS data, and the uncertainty of their estimate is not specified. We impose a constraint on global-mean surface ocean radiocarbon at the time of the acquisition of GEOSECS data of 11‰ with a standard error of ±11‰.

B9. Ocean Bomb-^{14}C Inventory

The ocean inventory of bomb-produced radiocarbon is considered an important constraint on the ocean uptake of CO_2. We use the recent estimate of 3.05×10^{28} atoms for January 1, 1975, which had a reported uncertainty (assumed standard error) of 10% [*Broecker et al*., 1995]. We assign a 90% confidence interval of 0.50×10^{28} atoms.

B10. Average Ocean ^{14}C Concentration

While the average ocean radiocarbon concentration will be correlated to some extent to the surface ocean $\Delta^{14}C$, its values is primarily dependent on deep sea $\Delta^{14}C$, and so we treat it as an independent constraint. The total ocean $\Delta^{14}C$ was estimated by *Oeschger et al*. [1975] to be 160‰, and this value is consistent [*Jain et al*., 1995, 1996; *Shaffer and Sarmiento*, 1995] with an integration of GEOSECS ocean average data with depth down to 4 km, the depth of the model ocean. We adopt a value of 160‰ with a standard error of this estimate of 5‰, roughly half that of the surface $\Delta^{14}C$.

B11. ^{14}C Ocean Plus Biosphere Inventory Change (1965–1990)

Over the period of nuclear weapons testing, radiocarbon has been injected primarily into the stratosphere. Estimates have been made of the changing production rate of bomb-produced radiocarbon, as well as observation-based estimates of the change in atmospheric inventory (troposphere plus stratosphere) over this period [*Broecker and Peng*, 1994; *Broecker et al*., 1995; *Hesshaimer et al*., 1994; *Jain et al*., 1996, 1997]. Conservation of radiocarbon dictates that the bomb production of radiocarbon minus the change in the atmospheric radiocarbon inventory is equal to the change in the ocean plus terrestrial biosphere inventories plus the decay of radiocarbon. There,

however, is great uncertainty in the rate of bomb production of radiocarbon based only on the cumulative explosive power of bombs [*Jain et al*., 1997]. Over the period following the nuclear weapons test ban (1963) the rate of testing dropped precipitously, decreasing the uncertainty in radiocarbon production over this period relative to the uncertainty in the change in atmospheric inventory. By 1965 the disequilibrium between the stratospheric and the tropospheric concentrations had, in large part, subsided, decreasing the uncertainty in the data-based estimate of total atmospheric radiocarbon inventory. We therefore use the {(bomb-^{14}C production) minus (change in atmospheric inventory)} over the period from 1965 to 1990 as a constraint on the model sinks of this radiocarbon which equal the {(bomb-^{14}C decay) plus (change in ocean ^{14}C inventory) plus (change in terrestrial biosphere ^{14}C inventory)}. For this quantity we use the value of 3.2×10^{28} atoms with a 90% confidence interval of $\pm 0.4 \times 10^{28}$ atoms estimated by *Jain et al*. [1997].

Acknowledgments. We thank Benjamin S. White for his advice on the application of Bayesian parameter estimation. The work of A. K. Jain and D. J. Wuebbles was supported, in part, by the U.S. Department of Energy Environmental Science Division (grant DOE DFG02-96ER 62284) and National Science Foundation (grant NSF DMF 9711624).

References

Andres, R. J., G. Marland, and S. Bischof, *The Carbon Isotopic Composition of Fossil Fuel Emissions*, Int. Union of Geod. and Geophys. (IUGG) XXI General Assembly, Boulder, Colo., 1995.

Bacastow, R., and C. D. Keeling, Atmospheric carbon dioxide and radiocarbon on the natural carbon cycle, in *Carbon and the Biosphere*, edited by G. M. Woodwell and E. V. Pecan, pp. 86–135, U.S. At. Energy Comm., Washington, D. C., 1973.

Brewer, P. G., Direct observation of the oceanic CO_2 increase, *Geophys. Res. Lett*., *5*, 997–1000, 1978.

Broecker, W. S., *How to Build a Habitable Planet*, Eldigio Press, Lamont-Doherty Geol. Obs., Palisades, N. Y., 1985.

Broecker, W. S., and T. H. Peng, *Tracers in the Sea*, Eldegio Press, Lamont-Doherty Geol. Obs., Palisades, N. Y., 1982.

Broecker, W. S., and T. H. Peng, Evaluation of the ^{13}C constraint on the uptake of fossil fuel CO_2 by the ocean, *Global Biogeochem. Cycles*, *7*, 619–626, 1993.

Broecker, W. S., and T.-H. Peng, Stratospheric contribution to the global bomb radiocarbon inventory: Model versus observation, *Global Biogeochem. Cycles*, *8*, 377–384, 1994.

Broecker, W. S., T.-H. Peng, and R. Engh, Modeling the carbon system, *Radiocarbon*, *22*, 565–580, 1980.

Broecker, W. S., T.-H. Peng, G. Ostlund, and M. Stuiver, The distribution of bomb radiocarbon in the ocean, *J. Geophys. Res*., *90*, 6953–6970, 1985.

Broecker, W. S., S. Sutherland, W. Smethie, T.-H. Peng, and G. Ostlund, Oceanic radiocarbon: Separation of the natural and bomb components, *Global Biogeochem. Cycles*, *9*, 263–288, 1995.

Bruno, M., and F. Joos, Terrestrial carbon storage during the past 200 years: A Monte Carlo analysis of CO_2 data from ice core and atmospheric measurements, *Global Biogeochem. Cycles*, *11*, 111–124, 1997.

Bullister, J. L., Chlorofluorocarbons as time-dependent tracers in the ocean, *Oceanography*, *2*, 12–17, 1989.

Chen, G.-T., and F. J. Millero, Gradual increase of oceanic CO_2, *Nature*, *277*, 205–206, 1979.

Ciais, P., P. P. Tans, M. Trolier, J. W. C. White, and R. J. Francey, A large Northern Hemisphere terrestrial CO_2 sink indicated by the $^{13}C/^{12}C$ ratio of atmospheric CO_2, *Science*, *269*, 1098–1102, 1995.

Craig, H., The natural distribution of radiocarbon and the exchange time of carbon dioxide between atmosphere and sea, *Tellus*, *9*, 1–17, 1957.

Doney, S. C., W. J. Jenkins, and H. G. Ostlund, A tritium budget for the North Atlantic, *J. Geophys. Res*., *98*, 18069–18081, 1993.

Druffel, E. M., Radiocarbon in annual coral rings of Florida and Belize, *Radiocarbon*, *22*, 363–371, 1980.

Druffel, E. M., Radiocarbon in annual coral rings from the eastern tropical Pacific Ocean, *Geophys. Res. Lett*., *8*, 59–62, 1981.

Druffel, E. M., and L. M. Benavides, Input of excess CO_2 to the surface ocean based on $^{13}C/^{12}C$ ratios in a banded Jamaican sclerosponge, *Nature*, *321*, 58–61, 1986.

Druffel, E. M., and T. W. Linick, Radiocarbon in annual coral rings of Florida, *Geophys. Res. Lett*., *5*, 913–916, 1978.

Duran, M. A., and B. S. White, Bayesian estimation applied to effective heat transfer coefficients in a packed bed, *Chem. Eng. Sci*., *50*, 495–510, 1995.

Enting, I. G., and G. I. Pearman, Description of a one-dimensional carbon cycle model calibrated by the techniques of constrained inversion, *Tellus*, *Ser. B*, *39*, 459–476, 1987.

Enting, I. G., T. M. L. Wigley, and M. Heimann (Eds.), *Future Emissions and Concentrations of Carbon Dioxide: Key Ocean/Atmosphere/Land Analyses*, 120 pp., Commonw. Sci. and Ind. Res. Organ., Melbourne, Victoria, Australia, 1994.

Friedli, H., H. Lotscher, H. Oeschger, U. Siegenthaler, and B. Stauffer, Ice core record of the $^{13}C/^{12}C$ ratio of atmospheric carbon dioxide in the past two centuries, *Nature*, *324*, 237–238, 1986.

Gruber, N., J. L. Sarmiento, and T. F. Stocker, An improved method for detecting anthropogenic CO_2 in the oceans, *Global Biogeochem. Cycles*, *10*, 809–837, 1996.

Harrison, K., W. Broecker, and G. Bonani, A strategy for estimating the impact of CO_2 fertilization on soil carbon, *Global Biogeochem. Cycles*, *7*, 69–80, 1993.

Harvey, L. D. D., Effect of model structure on the response of terrestrial biosphere models to CO_2 and temperature increases, *Global Biogeochem. Cycles*, *3*, 137–153, 1989a.

Harvey, L. D. D., Managing atmospheric CO_2, *Clim. Change*, *15*, 343–381, 1989b.

Heimann, M., and E. Maier-Reimer, On the relations between the oceanic uptake of CO_2 and its carbon isotopes, *Global Biogeochem. Cycles*, *10*, 89–110, 1996.

Hesshaimer, V., M. Heimann, and I. Levin, Radiocarbon evidence for a smaller ocean carbon dioxide sink than previously believed, *Nature*, *370*, 1994.

Hoffert, M. I., A. J. Callegari, and C.-T. Hseih, A box-diffusion carbon cycle model with upwelling, polar bottom water formation and a marine biosphere, in *Carbon Cycle Modeling, SCOPE 16*, edited by B. Bolin, pp. 287–305, John Wiley, New York, 1981.

Jain, A. K., H. S. Kheshgi, and D. J. Wuebbles, Integrated science model for assessment of climate change, *UCRL-JC-116526*, Lawrence Livermore Natl. Lab., Livermore, Calif., 1994.

Jain, A. K., H. S. Kheshgi, M. I. Hoffert, and D. J. Wuebbles, Distribution of radiocarbon as a test of global carbon cycle models, *Global Biogeochem. Cycles*, *9*, 153–166, 1995.

Jain, A. K., H. S. Kheshgi, and D. J. Wuebbles, A globally aggregated reconstruction of cycles of carbon and its isotopes, *Tellus*, *Ser. B*, *48*, 583–600, 1996.

Jain, A. K., H. S. Kheshgi, and D. J. Wuebbles, Is there an imbalance in the global budget of bomb-produced radiocarbon?, *J. Geophys. Res*., *102*, 1327–1333, 1997.

Joos, F., M. Bruno, R. Fink, U. Siegenthaler, T. Stocker, C. Le Quéré, and J. L. Sarmiento, An efficient and accurate representation of complex oceanic and biospheric models of anthropogenic carbon uptake, *Tellus*, *Ser. B*, *48*, 397–417, 1996.

Keeling, C. D., The carbon dioxide cycle: Reservoir models to depict the exchange of atmospheric carbon dioxide with the oceans and land plants, in *Chemistry of the Lower Atmosphere*, edited by S. I. Rasool, pp. 251–329, Plenum, New York, 1973.

Keeling, C. D., The modeling of rare isotopic carbon with regard to notation, in *Carbon Cycle Modeling, SCOPE 16*, edited by B. Bolin, pp. 89–94, John Wiley, New York, 1981.

Keeling, C. D., and T. Whorf, Trends in atmospheric CO_2 since the eruption of Pinatubo in 1991, in *4th International CO_2 Conference*, pp. 67–68, World Meteorol. Organ., Geneva, 1993.

Keeling, C. D., W. G. Mook, and P. Tans, Recent trends in the $^{13}C/^{12}C$ ratio of atmospheric carbon dioxide, *Nature*, *277*, 121–123, 1979.

Keeling, C. D., R. B. Bacastow, A. F. Carter, S. C. Piper, T. P. Whorf, M. Heimann, W. G. Mook, and H. Roeloffzen, A three-dimensional model of atmospheric CO_2 transport based on observed winds, 1, Analysis of observational data, in *Aspects of Climate Variability in the*

Pacific and Western Americas, *Geophys. Monogr. Ser*., edited by D. H. Peterson, pp. 165–236, AGU, Washington, D. C., 1989.
Keeling, C. D., T. P. Whorf, M. Wahlen, and J. v. d. Pilcht, Interannual extremes in the rates of rise of atmospheric carbon dioxide since 1980, *Nature*, *375*, 666–670, 1995.
Keeling, R. F., S. C. Piper, and M. Heimann, Global and hemispheric CO_2 sinks deduced from changes in atmospheric O_2 concentration, *Nature*, *381*, 218–221, 1996.
Kheshgi, H. S., and B. S. White, Modelling ocean carbon cycle with a nonlinear convolution model, *Tellus*, *Ser. B*, *48*, 3–12, 1996.
Kheshgi, H. S., M. I. Hoffert, and B. P. Flannery, Marine biota effects on the compositional structure of the world oceans, *J. Geophys. Res*., *96*, 4957–4969, 1991.
Kheshgi, H. S., A. K. Jain, and D. J. Wuebbles, Accounting for the missing carbon sink with the CO_2 fertilization effect, *Clim. Change*, *33*, 31–62, 1996.
Kheshgi, H. S., A. K. Jain, and D. J. Wuebbles, Analysis of proposed CO_2 emission reductions in the context of stabilization of CO_2 concentration, in *Proceedings of the A&WMA 90th Annual Meeting and Exhibition*, Air & Waste Manage. Assoc., Toronto, Ontario, Canada, 1997.
Kroopnic, P. M., The distribution of ^{13}C of ΣCO_2 in the world oceans, *Deep Sea Res*., *32*, 57–84, 1985.
Maier-Reimer, E., Geochemical tracers in an ocean general circulation model, Preindustrial tracer distributions, *Global Biogeochem. Cycles*, *7*, 645–677, 1993.
Maier-Reimer, E., and K. Hasselmann, Transport and storage of CO_2 in the ocean—An inorganic ocean-circulation carbon cycle model, *Clim. Dyn*., *2*, 63–90, 1987.
Marland, G., R. J. Andres, and T. A. Boden, Global, regional, and national CO_2 emissions, in *Trends 93: A Compendium of Data on Global Change*, edited by T. A. Boden et al., pp. 505–584, *ORNL/CDIAC-65*, Oak Ridge Natl. Lab., Oak Ridge, Tenn., 1994.
Mensh, M., A. Simon, and R. Bayer, Tritium and CFC input functions for the Weddell Sea, *J. Geophys. Res*., *103*, 15,923–15,937, 1998.
Neftel, A., E. Moor, H. Oeschger, and B. Stauffer, Evidence from polar ice cores for the increase in atmospheric CO_2 in the past two centuries, *Nature*, *315*, 45–47, 1985.
Nozaki, Y., D. M. Rye, K. K. Turekian, and R. E. Dodge, A 200 year record of carbon-13 and carbon-14 variations in a Bermuda coral, *Geophys Res. Lett*., *5*, 825–828, 1978.
O'Brien, K., Secular variations in the production of cosmogenic isotopes in the Earth's atmosphere, *J. Geophys. Res*., *84*, 423–431, 1979.
Oeschger, H., U. Siegenthaler, U. Schotterer, and A. Guglemann, A box-diffusion model to study the carbon dioxide exchange in nature, *Tellus*, *27*, 168–192, 1975.
Press, S. J., *Bayesian Statistics: Principles, Models, and Applications*, John Wiley, New York, 1989.
Quay, P. D., B. Tilbrook, and C. S. Wong, Oceanic uptake of fossil fuel CO_2: Carbon-13 evidence, *Science*, *256*, 74–79, 1992.
Sarmiento, J. L., U. Siegenthaler, and J. C. Orr, A perturbation simulation of CO_2 uptake in an ocean general circulation model, *J. Geophys. Res*., *97*, 3621–3645, 1992.
Schimel, D., I. Enting, M. Heimann, T. Wigley, D. Raynaud, D. Alves, and U. Siegenthaler, CO_2 and the carbon cycle, in *Climate Change 1994: Radiative Forcing of Climate Change and an Evaluation of the IPCC IS92 Emission Scenarios*, edited by J. T. Houghton et al., pp. 35–71, Cambridge Univ. Press, New York, 1995.
Schimel, D., D. Alves, I. Enting, M. Heimann, F. Joos, D. Raynaud, and T. Wigley, CO_2 and the carbon cycle, in *Climate Change 1995: The Science of Climate Change: Contribution of WGI to the Second Assessment Report of the IPCC*, edited by J. T. Houghton et al., pp. 65–86, Cambridge Univ. Press, New York, 1996.
Schlesinger, W., *Biogeochemistry: An Analysis of Global Change*, Academic, San Diego, Calif., 1991.
Shaffer, G., and J. L. Sarmiento, Biogeochemical cycling in the global ocean, 1, A new, analytical model with continuous vertical resolution and high-latitude dynamics, *J. Geophys. Res*., *100*, 2659–2672, 1995.
Siegenthaler, U., Uptake of excess CO_2 by an outcrop-diffusion model of the ocean, *J. Geophys. Res*., *88*, 3599–3608, 1983.
Siegenthaler, U., and F. Joos, Use of a simple model for studying oceanic tracer distributions and the global carbon cycle, *Tellus*, *Ser. B*, *44*, 186–207, 1992.
Siegenthaler, U., and K. O. Münnich, $^{13}C/^{12}C$ fractionation during CO_2 transfer from air to sea, in *Carbon Cycle Modeling, SCOPE 16*, edited by B. Bolin, pp. 249–257, John Wiley, New York, 1981.
Siegenthaler, U., and H. Oeschger, Biospheric CO_2 emissions during the past 200 years reconstructed by deconvolution of ice core data, *Tellus*, *Ser. B*, *39*, 140–154, 1987.
Siegenthaler, U., and J. L. Sarmiento, Atmospheric carbon dioxide and the ocean, *Nature*, *365*, 119–125, 1993.
Stuiver, M., and P. D. Quay, Changes in atmospheric ^{14}C attributed to variable Sun, *Science*, *207*, 11–19, 1980.
Stuiver, M., and P. D. Quay, Atmospheric ^{14}C changes resulting from fossil fuel CO_2 release and cosmic ray flux variability, *Earth Planet. Sci. Lett*., *53*, 349–362, 1981.
Suess, H. E., Radiocarbon concentration in modern wood, *Science*, *122*, 415–417, 1955.
Sundquist, E. T., Geological perspectives on carbon dioxide and the carbon cycle, in *The Carbon Cycle and Atmospheric CO_2: Natural Variations Archean to Present*, *Geophys. Monogr. Ser*., edited by E. T. Sundquist and W. S. Broecker, pp. 5–59, AGU, Washington, D. C., 1985.
Takahashi, T., W. S. Broecker, and A. E. Bainbridge, Supplement to the alkalinity and total carbon dioxide concentration in the world oceans, in *Carbon Cycle Modeling, SCOPE 16*, edited by B. Bolin, pp. 159–200, John Wiley, New York, 1981.
Tans, P., *Carbon-13 and Carbon-14 in Trees and the Atmospheric CO_2 Increases*, Univ. of Groningen, Netherlands, 1978.
Tans, P., $^{13}C/^{12}C$ of industrial CO_2, in *Carbon Cycle Modeling, SCOPE 16*, edited by B. Bolin, pp. 127–129, John Wiley, New York, 1981a.
Tans, P. P., A compilation of bomb ^{14}C data for use in global carbon cycle models, in *Carbon Cycle Modeling, Scope 16*, edited by B. Bolin, pp. 131–158, John Wiley, New York, 1981b.
Tans, P. P., J. A. Berry, and R. F. Keeling, Oceanic $^{13}C/^{12}C$ observations: A new window on ocean CO_2 uptake, *Global Biogeochem. Cycles*, *7*, 353–368, 1993.
Toggweiler, J. R., K. Dixon, and K. Bryan, Simulations of radiocarbon in a coarse resolution world ocean model, 1, Distributions of bomb-produced carbon-14, *J. Geophys. Res*., *94*, 8243–8264, 1989.
United Nations (UN), *United Nations Framework Convention on Climate Change*, New York, 1992.
Volk, T., Multi-property modeling of the marine biosphere in relation to global climate and carbon cycles, Ph.D. thesis, N.Y. Univ., Univ. Microfilms Int., Ann Arbor, Mich., 1984.
Volk, T., and M. I. Hoffert, Ocean carbon pumps: Analysis of relative strengths and efficiencies in ocean-driven atmospheric CO_2 changes, in *The Carbon Cycle and Atmospheric CO_2: Natural Variations Archean to Present*, *Geophys. Monogr. Ser*., edited by E. Sundquist and W. S. Broecker, pp. 91–110, AGU, Washington, D. C., 1985.
Volk, T., and Z. Liu, Controls of CO_2 sources and sinks in the Earth scale surface ocean: Temperature and nutrients, *Global Biogeochem. Cycles*, *2*, 73–89, 1988.
Watson, R. T., H. Rodhe, H. Oeschger, and U. Siegenthaler, Greenhouse gases and aerosols, in *Climate Change, The IPCC Scientific Assessment*, edited by J. T. Houghton et al., pp. 1–40, Cambridge Univ. Press, Cambridge, New York, 1990.
Wigley, T. M. L., Balancing the carbon budget, Implications for projections of future carbon dioxide concentration changes, *Tellus*, *Ser. B*, *45*, 409–425, 1993.

A. K. Jain and D. J. Wuebbles, Department of Atmospheric Sciences, University of Illinois, Urbana, IL 61801.

H. S. Kheshgi, Corporate Research Laboratories, Exxon Research and Engineering Company, Annandale, NJ 08801. (hskhesh@erenj.com)

(Received February 15, 1999; revised June 8, 1999;
accepted September 15, 1999.)